APL Materials

Electrolyte-gated magnetoelectric actuation: Phenomenology, materials, mechanisms, and prospective applications

Cite as: APL Mater. **7**, 030701 (2019); https://doi.org/10.1063/1.5080284
Submitted: 07 November 2018 . Accepted: 01 January 2019 . Published Online: 06 March 2019

Cristina Navarro-Senent, Alberto Quintana, Enric Menéndez, Eva Pellicer, and Jordi Sort

Electrolyte-gated magnetoelectric actuation: Phenomenology, materials, mechanisms, and prospective applications

Cite as: APL Mater. 7, 030701 (2019); doi: 10.1063/1.5080284
Submitted: 7 November 2018 • Accepted: 1 January 2019 •
Published Online: 6 March 2019

Cristina Navarro-Senent,[1] Alberto Quintana,[1] Enric Menéndez,[1] Eva Pellicer,[1] and Jordi Sort[1,2,a)]

AFFILIATIONS

[1]Departament de Física, Universitat Autònoma de Barcelona, E-08193 Cerdanyola del Vallès, Spain
[2]Institució Catalana de Recerca i Estudis Avançats (ICREA), Passeig Lluís Companys 23, E-08010 Barcelona, Spain

[a)]Author to whom correspondence should be addressed: Jordi.Sort@uab.cat

ABSTRACT

Manipulation of the magnetic behavior of materials with voltage (i.e., magnetoelectric actuation) has become a topic of intense research during the last years. Apart from its obvious interest from a basic science standpoint, control and eventual switching of the magnetization without applying any external magnetic field (or spin polarized current) has the potential to drastically reduce the power consumption of magnetic devices due to the lack (or minimization) of Joule heating dissipation effects. Herein, an overview of the state-of-the-art of electrolyte-gated magnetoelectric actuation (where an electric field is applied using an electrolyte, either liquid or solid) is provided. The different types of mechanisms responsible for voltage-driven magnetic actuation (surface charging, ionic migration, also termed "magneto-ionics," reduction/oxidation reactions, and ferroelectric/ferromagnetic coupling) are summarized. The various effects (changes in coercivity, anisotropy easy axis, exchange bias field, saturation magnetization, Curie temperature, etc.) observed in the different types of materials investigated so far (mainly metallic thin films and semiconductors, porous alloys, and nanocomposite structures) are described. The potential applications of electrolyte-gated magnetoelectric actuation in devices as well as the current challenges in the field are also reviewed with the aim of providing the basic ingredients for further prospects and technological advancements in this area.

I. INTRODUCTION

Magnetic devices, such as micro-/nano-electromechanical systems (MEMS/NEMS), computer hard disks, magnetoresistive random-access memories (MRAMs), or spintronic systems, are conventionally operated using magnetic fields. In conventional recording media, such magnetic fields are generated with electromagnets in which relatively high electric currents are involved.[1] In MRAMs, the spin switching is also achieved by passing a current through a neighboring metallic strip which generates the magnetic field. Recently, spin-polarized electric currents are being used to orient the magnetic bits in magnetic memories via spin-transfer torque.[2] In all these cases, due to the presence of flowing currents, a large fraction of the energy employed to control magnetization is wasted in the form of heat dissipation by the Joule effect. For this reason, there is a growing interest in finding alternative methodologies to process magnetic information and operate magnetic/spintronic devices using voltage (or electric field), instead of electric currents.

The grounds of the magnetoelectric effect (ME) were postulated already in 1894 by Curie[3] although the first experimental observations date from 1960.[4] The magnetoelectric effect refers to the influence of an external magnetic field on the electric polarization of certain materials or, conversely, the effect of the external electric field on the magnetic properties of materials. A traditional approach to tailor magnetism by means of voltage is to take advantage of strain-mediated magnetoelectric coupling in piezoelectric-magnetostrictive hybrid materials. In such systems, the applied electric field

induces strain in the piezoelectric counterpart, which is transferred to the magnetic material, causing changes in the orientation of its net magnetic moment via the inverse magnetostriction or Villari effect.[5] This effect has been successfully exploited in transducers, magnetic actuators, and a variety of other hybrid devices.[6–9] However, in spintronic devices, this approach has some disadvantages. First, in thin films, there is a reduced piezoelectric response due to the clamping with the substrate. In addition, repetitive strain action may ultimately cause mechanical fatigue and device failure. There have been some attempts to induce magnetoelectric effects in single-phase materials exhibiting simultaneously magnetic and electric coupled ferroic orders, also known as "multiferroics."[10] Unfortunately, despite intensive recent efforts, most single phase multiferroic materials consist of complex oxides that exhibit their properties basically at low temperatures (with a few exceptions[11]). Therefore, there is a technological demand for alternative approaches to manipulate magnetism with electric field at room temperature.

About two decades ago, several studies showed the possibility to modify the magnetic properties of diluted magnetic semiconductors directly with electric field, without strain-mediated effects, due to the changes induced in the carrier density (donors or holes) which mediate the exchange interactions responsible for the onset of ferromagnetism in these materials.[12,13] As a result, variations in coercivity (H_C), Curie temperature (T_C), magnetization (M), or magnetic easy axis were reported when applying electric fields of the order of 0.5–5 V/Å. Such effects in semiconductors occur at penetration depths within the Debye radius, which is around 10–12 nm. Inspired by these studies, similar observations were later made on ultra-thin magnetic metallic films.[14–16] However, in metals, the electric field is more effectively screened than in semiconductors and electric charges are accumulated just at the surface, near the interface with the dielectric material employed to generate the electric field (within the Thomas-Fermi screening length which is around 0.5 nm).[17] These charges can alter the wave function and the occupancy of the *d* orbitals of the alloy, eventually inducing changes in the magnetic properties since the electric field screening depends on the orientation of the spin. It should be noted that although the electric field is only effective at the very surface of the alloy, the induced magnetic changes can propagate up to 20 nm toward the interior of the alloy, due to the spin-spin exchange correlation length. Given the high surface area-to-volume ratio of nanoporous materials, magnetoelectric effects ascribed to electric charge accumulation have been recently observed in relatively thick (few hundred nm thickness) nanoporous metallic films (e.g., Cu-Ni,[18] Fe-Cu[19]) with ultra-narrow pore walls (~5 nm), prepared by advanced electrodeposition procedures.

Besides strain and electric surface charging, voltage can also induce changes in the oxidation state of ferromagnetic (FM) metallic alloys (i.e., reduction/oxidation reactions or oxygen ion migration), particularly when these alloys are immersed in aqueous electrolytes or grown in direct contact with an ionically conducting oxide buffer layer (i.e., solid electrolyte).[12–24] This approach was first carried out by immersing metallic films and nanoporous metallic alloys in aqueous electrolytes.[20–22] Subsequent studies showed the possibility to modify the magnetic properties of metal/metal oxide heterostructures[23,24] or even oxide materials (e.g., Fe_2O_3, Co_3O_4) with voltage when immersing them either in aqueous[25] or even non-aqueous[26] electrolytes, in all cases assisted by redox reactions or O^{2-} ion motion. In the solid state, O^{2-} can diffuse back and forth from the material of interest toward an oxygen source/sink (e.g., a high O^{2-} mobility thin film, such as HfO_2 or Gd_2O_3, deposited next to the FM layer), depending on the voltage polarity.[27–32] Interestingly, not only oxygen migration but also cationic movement has been reported.[33] Alternatively, the properties of FM or ferrimagnetic oxides have also been tuned by voltage-driven lithiation (Li^+ incorporation using suitable electrolytes).[34–37] These effects have been sometimes referred to as "electrochemical reactions" or "magneto-ionic effects" although these reactions are typically not restricted to the surface but can affect a significant fraction of the overall film thickness, depending on the experimental conditions and the ability of the system to trigger ion migration. In any case, magneto-ionics has gained huge interest recently since the induced effects are non-volatile. This is opposite to simple charge accumulation, where the magnetic changes instantaneously disappear when voltage is removed unless a ferroelectric (FE) layer (with high remanent electric polarization) is used as a dielectric. Despite being non-volatile, the effects caused by ion migration can be partially or totally reversed when the sign of the electric field is inverted. Electrochemical processes also overcome one of the main drawbacks of pure charge accumulation, i.e., the limited depth in which the phenomenon occurs due to the electric field screening length. Hence, electrochemical reactions are observable even in relatively thick films. One of the drawbacks of electrochemical processes is, nevertheless, that the effects are not induced instantaneously (until today, the dynamics is relatively slow, taking place in minutes or hours, as will be described in Sec. III), hampering the utilization of magneto-ionics in high-speed memory applications and spintronics.

Usually, all the aforementioned mechanisms (see Fig. 1 for an overview of these mechanisms) do not occur separately in voltage-actuated magnetic materials. In most cases, various effects act synergistically to tailor the magnetic behavior under the action of an electric field and it is difficult to discriminate between them. The influence of electric charging on the various magnetic properties of thin films, multilayers, and nanostructures has been reviewed to some extent from a theoretical point of view by Brovko *et al.*[38] In turn, Song *et al.*[39] recently reviewed the general mechanisms responsible for voltage control of magnetism. Fusil *et al.*[40] also summarized the different applications of magnetoelectric materials (with special emphasis in multiferroics) in spintronics. Here we focus on the most relevant studies dealing with electrolyte-gating as a means to generate ultra-high electric fields (resulting in huge magnetoelectric effects) and the new types of materials, electrolytes, and experimental configurations that have led to unprecedented results on magnetoelectric actuation of materials during the last fewyears.

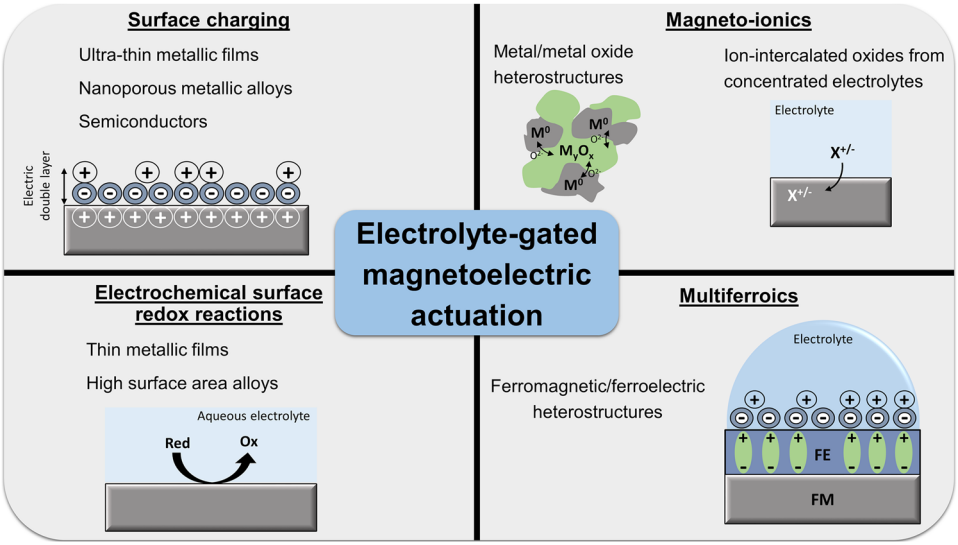

FIG. 1. Main mechanisms responsible for electrolyte-gated magnetoelectric actuation. The most representative types of materials for each case are indicated, together with simple drawings to illustrate the physical/physicochemical principles governing each mechanism.

II. EXPERIMENTAL CONFIGURATIONS AND MAGNETOELECTRIC MEASUREMENT TECHNIQUES: SOLID DIELECTRIC LAYERS *VS.* ELECTRIC DOUBLE LAYERS

To apply an electric field on magnetic materials, two main geometries are commonly utilized. The first one is the field effect transistor (FET) structure, consisting of a source electrode, a drain electrode, and a gate electrode [Fig. 2(a)] in which magnetic properties are typically (but not always) assessed by resistive Hall effect measurements. Here the gate voltage is the one that alters the magnetic properties of the FM layer, and the current flowing from the source to the drain is used to track the changes in M. The gate electrode and the FM layer are isolated by an insulating (dielectric) layer. Another convenient geometry is the condenser-like structure [Fig. 2(b)]. In this case, the FM material is grown on top or below an insulating layer and voltage is applied between the FM material and the counter-electrode grown on the other side of the dielectric layer.

The strength of the electric fields needed to modify the magnetic properties of materials typically falls in the range between 0.01 V/Å and 5 V/Å. To obtain these fields, relatively large voltages need to be applied (sometimes of the order of tens or hundreds of V), unless the electrically insulating layers are made extremely thin. The charge accumulated in a condenser is Q = ΔV C, where C is the capacity and ΔV is the applied voltage. In turn, $C = \varepsilon_r \varepsilon_0 A/d$, where ε_r is the relative permittivity, ε_0 is the vacuum permittivity, A is the area of the plates, and d is the thickness of the dielectric layer. Hence, the accumulated charge for a given voltage-actuated material can be given as

$$Q = \Delta V \varepsilon_r \varepsilon_0 A/d. \quad (1)$$

Generation of hundreds of V is, of course, not very convenient for practical applications. Hence, ultra-thin dielectrics are desirable. However, despite the recent progress in deposition techniques, such as sputtering, molecular beam epitaxy, or atomic layer deposition, the production of solid-state devices with high-quality ultra-thin dielectric layers (e.g., 1–2 nm thick Al_2O_3, SiO_2, HfO_2, or MgO) is still very challenging since the presence of structural defects easily result in pinholes through which the accumulated electric charges tend to leak. Several approaches have been engineered to tackle this problem. The first one is the utilization of insulating polymers such as polyimide (PI) or polyvinyl difluoride (PVDF).[41,42] However, making these polymers very thin (by, e.g., spin coating) is not straightforward and, anyhow, the voltage they can afford without dielectric breakdown is also rather limited. A second approach is to employ liquid electrolytes. This includes (i) polar aprotic organic solvents (such as ethylene carbonate or propylene carbonate) and (ii) ionic liquids [e.g., diethylmethyl(2-methoxyethyl)ammonium bis(trifluoromethylsulfonyl)imide (DEME-TFSI), 1-ethyl-3-methylimidazolium bis(trifluoromethylsulfonyl)imide (EMIM-TFSI or EMI-TFSI)] or other electrolytes such as $LiPF_6$ dissolved in ethylene carbonate or $KClO_4$-polyethylene oxide as a means to generate the electric field. Aqueous electrolytes

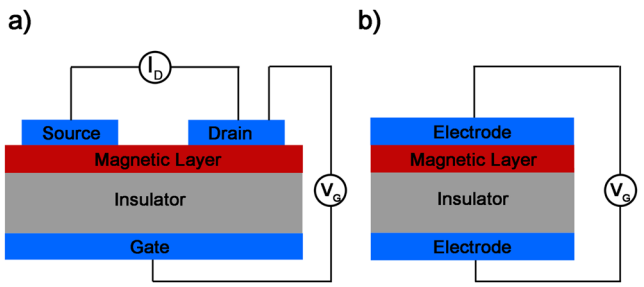

FIG. 2. Schematic drawings of the (a) field-effect transistor and (b) condenser-like geometry employed to apply electric fields on magnetic materials.

TABLE I. Representative materials, typical electrolytes, and most prominent magnetoelectric effects induced by "pure" surface charging (electrostatic surface charge accumulation). Note that the following acronyms are used in the table: PC: propylene carbonate; $LiClO_4$: lithium perchlorate; EC: ethylene carbonate; DEME-TFSI: N,N-diethyl-N-(2-methoxyethyl)-N-methylammonium bis(trifluoromethylsulfonyl)-imide; $CsClO_4$: cesium perchlorate; PEO: polyethylene oxide; EMI-TFSI: 1-ethyl-3-methylimidazolium bis(trifluoromethylsulfonyl)imide; P(VDF-HFP): poly(vinylidene fluoride)-poly(vinylidene fluoride-co-hexafluoropropylene); H_C: coercivity; PM: paramagnetic; FM: ferromagnetic; T_C: Curie temperature; M_R: remanent magnetization; DW velocity: domain wall velocity; PMA: perpendicular magnetic anisotropy; FM-HMI transition: ferromagnetic-hard magnetic insulating transition; MAE: magnetic anisotropy energy; M: magnetization; H_R: resonance field (ferromagnetic resonance experiments).

Electrolyte	Material	Magnetic parameter	Variation	Reversibility	References
PC	Fe-Pt and Fe-Pd ultra-thin films	H_C	−4.5% (FePt) +1% (FePd)	Yes (ΔV, ~5 min)	14
PC	Co-Pd film	M	≈ 4.5%	...	50
$LiClO_4$ in EC	Nanoporous Au-Fe alloy	M	0.2%	Yes	53
$LiClO_4$ in EC	Nanoporous Pd-Ni alloy	M	≈ 0.5 % ($Pd_{74}Ni_{26}$) ≈ 0.3% ($Pd_{35}Ni_{65}$)	Partially (ΔV, ~1 h) Yes (ΔV, ~1 h)	55
DEME-TFSI $CsClO_4$ in PEO	$(Ti,Co)O_2$ film	M	PM-FM switching	...	49
EMI-TFSI	Co ultra-thin film	T_C M_R H_C	$\Delta T_C \approx +17\%$ −14%	Yes (ΔV, 0.5–1 h)	59
EMI-TFSI	Fe-Pt/Al_2O_3 film	Domain walls	Domain wall propagation	Yes (ΔV, ~min)	60
EMI-TFSI	CoFeB/MgO film	Domain walls H_C	ΔDW velocity = 4.2 factor ΔH_C = 1.3 factor	Yes (ΔV, ~s)	62
DEME-TFSI	LSMO ultra-thin film	T_C M	PM–FM switching ΔT_C = 14–26 K ΔM = 98.5%–128%	Yes (ΔV, ~min)	65
PC	Nanoporous Cu-Ni film	H_C	−32%	...	18
PC	Pseudo-ordered porous FeCu film	H_C	−25%	Partially (0 V, 5 min)	19
$LiClO_4$ in EC	Nanoporous Pd-Co alloy	M	3%	Partially (ΔV, ~2 h)	56
EMI-TFSI	CoFeB/MgO/HfO_2 ultra-thin film	PMA DW velocity	$\Delta PMA = 0.108\ mJ/m^2$	Yes (0 V, slow time)	61
$LiClO_4$ in PC	Nanoporous LSMO	M	1.8%–2.5%	Yes (ΔV, ~h)	63
DEME-TFSI	LSMO film	T_C FM-HMI transition	$\Delta T_C \approx 21\%$	...	64
EMI-TFSI in PVDF	$(Pt/Co)_2/Pt$ film	MAE	$3.16 \times 10^5\ J/m^3$	Yes (0 V, -)	67
EMI-TFSI in P(VDF-HFP)	Pt/Fe/Pt film	Anisotropy field	ΔH_R = 114 Oe	Yes (ΔV, ~min)	68

TABLE II. Representative materials, typical electrolytes, and most prominent magnetoelectric effects induced by surface reduction/oxidation reactions. The following acronyms are used in the table: KOH: potassium hydroxide; NaOH: sodium hydroxide; $LiClO_4$: lithium perchlorate; DMC: dimethyl carbonate; EC: ethylene carbonate; MAE: magnetic anisotropy energy; m: magnetic moment; M_S: saturation magnetization; $R_{AH,S}$: anomalous Hall resistivity at saturation; M: magnetization.

Electrolyte	Material	Magnetic parameter	Variation	Reversibility	References
1M KOH	Nanoporous Pd-Ni alloy	M	24.6%	Yes (ΔV, ~2 h)	21
0.01M KOH	Co ultra-thin film	MAE	$0.36\ erg/cm^2$	...	20
1M KOH	γ-Fe_2O_3/Pt-nanocomposite	M	4.2%	Yes (ΔV, ~min)	25
1M KOH	Fe-O/Fe films	M	64%	Partially (ΔV, -)	24
	Fe_3O_4/Fe/(001) $L1_0$ FePt ultra-thin film	M_R/M_S PMA MAE	MAE = 55%		
0.001M–6M KOH	Fe film	M_S	20%	...	22
1M NaOH	Nanoporous Cu-Ni	M_S	+33%	Yes (ΔV, 10 min)	72
1M KOH	FeO_x/Fe nanoislands	M	$\Delta M_S \approx \Delta R_{AH,S}$ = +86%	Yes (ΔV, -)	23
1M KOH	Porous γ-Fe_2O_3/Pt-nanocomposite	M	Δm = 10.4%	Yes (ΔV, ~5 min)	71
$LiClO_4$ in DMC/EC	CoPt ultra-thin films	H_C M_S	ΔH_C = +200% ΔM_S = +4%	No	73

(with dissolved KOH or NaOH) are also utilized when the aim is only to induce voltage-driven redox reactions on the magnetic material immersed in the solution. The different types of electrolytes together with the main experimental observations on various types of voltage-controlled magnetic materials are summarized in Tables I–III.

In liquid electrolytes, low voltages can generate reasonably high electric fields due to the formation of the "electric double layer" (EDL), which is extremely thin. Electric fields of the order of hundreds of MV/cm can be reached applying moderate voltages.[18] The EDL is simply the solid-liquid capacitor formed between a solid electrode and dissolved ions in close proximity with a solvent acting as a dielectric.[43] The Gouy–Chapman–Stern is the most popular theory to model the EDL capacitance and to study the ionic dynamics at electrode/electrolyte interfaces.[44] A flat EDL is created by

TABLE III. Representative materials, typical electrolytes, and most prominent magnetoelectric effects induced by voltage-driven ion migration (magneto-ionics), including ion incorporation from the electrolytes. The following acronyms are used in the table: EMI-TFSA: 1-ethyl-3-methylimidazolium and bis(trifluoromethylsulfonyl)amide; P(VDF-HFP): poly(vinylidene fluoride-co-hexa-fluoropropylene); DEME-TFSI: N,N-diethyl-N-(2-methoxyethyl)-N-methylammonium bis(trifluoromethylsulfonyl)-imide; $TMPA^+/TFSI^-$: N,N,N-trimethyl-N-propylammonium/bis(trifluoromethylsulfonyl)imide; $LiPF_6$: lithium hexafluorophosphate; LiTFSI: lithium bis(trifluoromethanesulfonyl)imide; DMC: dimethyl carbonate; EC: ethylene carbonate; DEC: diethyl carbonate; PC: propylene carbonate; T_C: Curie temperature; M_S: saturated magnetization; H_C: coercivity; H_E: exchange bias field; $R_{AH,S}$: anomalous Hall resistivity at saturation; MA: magnetic anisotropy; T_B: superparamagnetic blocking temperature; T_t: transition temperature; H_R: ferromagnetic resonance field; K_{eff}: effective anisotropy constant; MAE: magnetic anisotropy energy; M_R/M_S: remanence to saturation magnetization ratio; DW velocity: domain wall velocity; M: magnetization.

Electrolyte	Material	Magnetic parameter	Variation	Reversibility	References
EMI-TFSA in P(VDF-HFP)	$SrRuO_3$ film	T_C	ΔT_C = 30 K	Yes (ΔV, -)	89
DEME-TFSI	Co/Ni/HfO_2 films	M_S PMA T_C	$\Delta M_S \approx$ +11%–21% −53% $\Delta T_C \approx$ 10%	Yes (ΔV, ~30 min)	31
DEME-TFSI	Co/Ni/HfO_2 films $[Co/Ni]_3/HfO_2$ films	M_S H_E H_C	$\Delta M_S \approx \Delta R_{AH,S}$ = +70% ΔH_E, ≈ 54% $\Delta H_C \approx$ 74%	Yes (ΔV, ~10 min) Partially (ΔV, ~30 min)	32
MaN2401	Co ultra-thin film	H_C	ΔH_C ~ 68%	Yes (ΔV, ~30 min)	81
DEME-TFSI	FeRh/HfO_2 film	T_t	$T_{t\text{-warm}} \approx$ −10% $T_{t\text{-cool}} \approx$ −31%	Yes (ΔV, -)	82
DEME-TFSI	Co ultra-thin film	MA	ΔH_R = 219 Oe	Yes (ΔV, 5 min)	85
$TMPA^+/TFSI^-$	Cu/Ni ultra-thin films	T_B	ΔT_B = 28 °C	Yes (ΔV, -)	86
DEME-TFSI	$SrCoO_{3-\delta}$, $SrCoO_{2.5}$, and $HSrCoO_{2.5}$ films	Phase transition	FM insulator-FM metal-AFM insulator phase transition	Yes (ΔV, ~min)	90
DEME-TFSI	$Pr_{0.65}(Ca_{0.75}Sr_{0.25})_{0.35}MnO_3$ films	Phase transition	FM fraction (~±0.15%)	Yes (ΔV, -)	96
$LiPF_6$ in DMC/EC	Fe-Pt ultra-thin films	M_S	$\Delta M_S \approx \Delta R_{AH,S}$ = 8%	Yes (ΔV, -)	98
$LiPF_6$ in DMC/EC	FePt/iron oxide composites	M_S K_{eff}	ΔK_{eff} = −25% $\Delta M_S \approx \Delta R_{AH,S}$ = +4%	Yes (ΔV, -)	99
$LiPF_6$ in EC/DEC	γ-Fe_2O_3 nanoparticles	M	$\Delta m \approx$ 20 Am^2/kg	Yes (ΔV, ~h)	100
LiTFSI in EMIM-TFSI	Nanoporous $Co_{0.5}Ni_{0.5}Fe_2O_4$ and $CoFe_2O_4$ films	M	$\Delta M \approx$ 2.5%–5 %	Yes (ΔV, ~min)	101
LiTFSI in EMIM-TFSI	Nanoporous α-$LiFe_5O_8$ films	M	$\Delta M \approx$ 4%	Yes (ΔV, ~h)	102
$LiPF_6$ in PC	Nanoscale α-Fe_2O_3-based film	M_S H_C	$\Delta M_s \approx$ 157.14 emu/g $\Delta H_C \approx$ 134.4 Oe	Yes (ΔV, -)	34
PC	Co_3O_4 film	Magnetic transition	FM–PM transition	Yes (ΔV, 1 h)	72
GdO_x	Co/GdO_x ultra-thin films	MAE M_R/M_S H_C	0.75 erg/cm^2	Yes (ΔV, 10 s)	28
GdO_x	AlO_x/GdO_x/Co films	M	−80% (interface) −38% (bulk)	Partially (ΔV, 40 min)	29
AlO_x	Co/AlO_x ultra-thin film	Domain wall velocity	From 0.4 to 4 μm/s	...	75
PC	Nanoporous Fe-Cu films	M_S H_C	ΔM_S = 20% ΔH_C = 100%	Partially (ΔV, 40 min)	87
EMI-TFSI in P(VDF-HFP)	LSCO ultra-thin film	T_C	ΔT_C = 7%	...	92

a charged plane in contact with an electrolyte solution composed of solvent molecules, counter-ions (ions with the charge of the opposite sign than the plane), and co-ions (ions with the charge of the same sign as the plane) [see Fig. 3(a)].[45] A buildup of counter-ions near the surface creates an excess electric potential in the surface neighborhood. This effect is particularly pronounced when a polar medium is used, wherein the surface charges of the solid attract counter-ions distributed in the polar solvent.[46] This potential drops over some distance, from the value at the surface to some lower Galvani potential in the bulk of the solution. The effective thickness of the EDL increases with increasing counter-ion size and with decreasing bulk concentration of ions, whereas either a decrease or increase in the effective thickness may be caused by an increase in the surface charge. The distance from a solid flat surface to the inner Helmholtz plane is around the order of one bare ionic radius, roughly 0.1 nm, while that to the outer Helmholtz plane is roughly one hydrated ionic radius, about 0.5 nm.[47] The diffuse layer can extend a few nm from the surface of the electrode. When non-flat surfaces are involved, as would be the case of nanoporous materials [Fig. 3(b)], the structure of the EDL becomes more complex, being influenced by entropy effects and resulting in non-homogeneous potential distributions.[48]

To perform magnetoelectric measurements using liquid electrolytes, conventional magnetometry techniques such as the magneto-optic Kerr effect (MOKE), superconducting quantum interference device (SQUID), or vibrating sample magnetometry (VSM) are typically assembled together with electrolytic cells that allow for *in situ* application of voltage while hysteresis loops are being recorded (see Fig. 4). Although not straightforward, *in situ* structural characterization of the investigated materials under an applied electric field is sometimes performed in order to elucidate the mechanism responsible for the observed changes in magnetic properties. In most cases, though, the materials are structurally characterized *ex-situ* (i.e., after voltage removal). This is useful only when voltage causes permanent changes in the structure of the films (e.g., magneto-ionics or redox reactions).

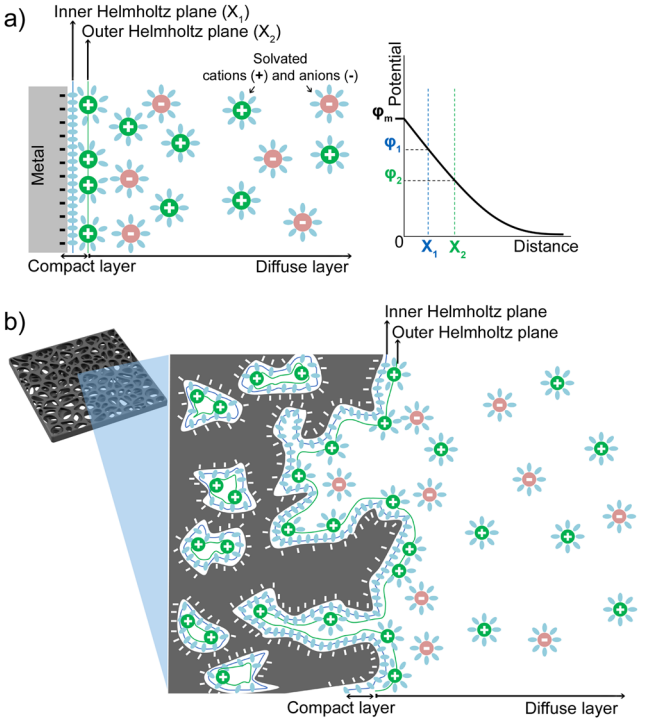

FIG. 3. Schematic representation of the formation of the electric double layer (ELD) onto the surface of (a) a flat electrode and (b) a nanoporous electrode.

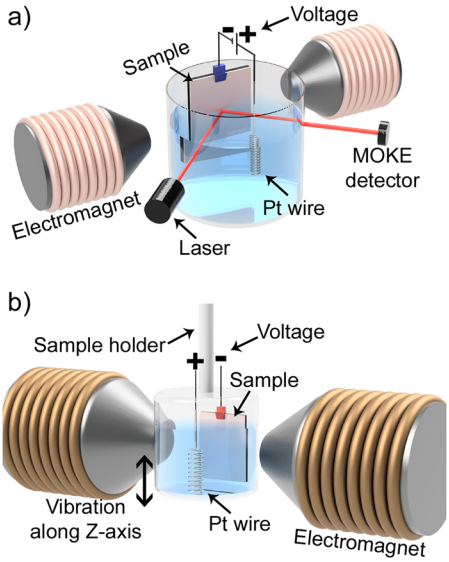

FIG. 4. Schematic illustration of the experimental setups typically used for magnetoelectric measurements in a liquid configuration using (a) a magneto-optic Kerr effect setup (MOKE) and (b) a vibrating sample magnetometer (VSM).

III. MATERIALS AND MAIN EXPERIMENTAL OBSERVATIONS

The vast majority of materials used in electrolyte-gated magnetoelectric experiments are prepared in the form of thin films (sometimes lithographed) using sputtering, pulse laser deposition (for oxides), or electrodeposition (for metals or semiconductors) (see Fig. 1). Ultra-thin metallic films (0.5–4 nm) or nanoporous alloys (both with very high surface area-to-volume ratio) are required to observe pure surface charging effects since the accumulated carrier density is proportional to the overall surface area [Eq. (1)]. Oxygen ions' migration and redox reactions are generally promoted when the alloys are immersed in protic solvents that can provide oxygen to the magnetic system. Magneto-ionic effects can be also observed in systems where the magnetic layer is put in direct contact with oxide layers (e.g., HfO_2, Gd_2O_3) that can absorb or release oxygen to the magnetic material under voltage application (i.e., acting as solid electrolytes). Also interesting are the magnetoelectric effects originating from the

coupling between FE and FM layers, sometimes exacerbated by using ionic liquids. In the following, the main types of electrolyte-gated materials and magnetoelectric observations due to charge accumulation, redox, magneto-ionic phenomena, and FE/FM coupling, in all cases assisted or mediated by liquid or solid electrolytes, are summarized.

A. Pure charge accumulation magnetoelectric effects

Pioneering studies on electric field manipulation of the magnetic properties due to charge accumulation were carried out on diluted magnetic semiconductors (DMSs). Specifically, Ohno and co-workers[12] successfully modified T_C in a (In, Mn)As ultra-thin film (4 nm), taking advantage of the hole-dependent ferromagnetism of this system. Upon application of an electric-field of ±1.56 MV/cm, which corresponds to a change in the carrier density of the order of 10^{-12} cm^{-1}, the authors successfully tuned T_C by ∓2 K. Changes in H_C and the anisotropy easy axis direction were observed in a similar DMS subject to voltage, where an electric field was applied through a solid dielectric layer using a FET configuration.[13] Despite the promising results shown in these preliminary studies, the low temperature character of the magnetic properties of DMS made it necessary to move toward more robust, room temperature FM materials, such as high-T_C oxide diluted magnetic semiconductors[49] or metallic magnetic materials, where the use of an electrolyte can further assist and improve the magnetoelectric effect on such systems.

A huge breakthrough was achieved by Weisheit *et al.*[14] who observed the first surface charging magnetoelectric effect in metallic ultra-thin films. The authors were able to tune the H_C of FePt and FePd films by a factor of 4.5% and 1%, respectively. The trends for FePt and FePd were opposite for the same applied voltage, which was a strong confirmation for the theoretical predictions about this magnetoelectric effect being directly linked to the material's band structure. To apply a sufficiently high electric field without leakage currents, EDL gating using propylene carbonate with dissolved Na^+ and OH^- ions was employed. The reported changes were thickness-dependent, evidencing the surface character of the phenomenon. The observed changes in H_C were attributed to voltage-driven variations in the magnetic anisotropy energy (MAE). This work can be considered as a seminal one concerning voltage-actuation of metallic materials, and several studies focused on "surface charging" effects in magnetic materials followed afterwards (see Table I).

While Weisheit *et al.* reported changes in H_C which almost vanished in a 4 nm thick film, Zhernenkov *et al.*[50] reported changes in M in a thicker (18.5 nm) CoPd film. Since Kerr spectroscopy cannot provide depth resolution and quantitative assessment of M, the authors employed polarized neutron reflectivity to evaluate the M profile as a function of depth. Gating was also performed using propylene carbonate. An enhancement of M, scaling linearly with the applied voltage, was observed within approximately 7 nm from the surface of the film. This thickness is much larger than in the case of FePt or FePd.[14] The affected region is, in fact, of the order of the magnetic exchange length for CoPd, thus suggesting that, upon charging, a perturbation in the Fermi level occurs and, due to the spin-spin exchange coupling, the effect is then propagated.

The influence of applied voltage on "magnetic proximity effects" was investigated by Obinata *et al.*[51] in a Pd film deposited onto a FM Co/Pt bilayer gated using an ionic liquid electrolyte. The surface magnetic moment induced by the proximity effect on the polarized Pd layer could be tailored by the external voltage. The electric field supposedly induced changes in the density of states at energy levels close to the Fermi level, hence modifying the net moment of Pd. Quite recently, ionic liquid gating has been also shown to induce changes in the Ruderman–Kittel–Kasuya–Yosida (RKKY) interaction in FeCoB/Ru/FeCoB and [Pt/Co]/Ru/[Pt/Co] multilayers as a result of a voltage-induced disturbance of itinerant electrons inside the synthetic antiferromagnetic heterostructures and the concomitant change in the Fermi energy level.[52] This resulted in pronounced changes in the overall shapes of the hysteresis loops for applied voltages of the order of a few V.

Controlled reversible changes in M (0.1%–0.2%) were also reported as a function of voltage in porous Au-Fe alloys immersed in lithium perchlorate dissolved in ethylene acetate.[53] The observed effect was partially ascribed to the Coulomb pressure effect (i.e., voltage-induced strain[54]) due to the surface charging. It should be noted that the pore wall thickness in this material is close to 50–100 nm; hence, variations in the MAE ascribed to pure charging are anticipated to be very small. By using the same electrolyte, Ghosh *et al.*[55,56] were also able to alter the magnetic properties of porous Pd-Ni and Pd-Co alloys, in a reversible manner, but again to a rather limited extent (a few % variation in M). The effect was again attributed to elastic strain due to disturbance of atomic bonding with the excess charge accumulated on the metal surface (i.e., magnetoelastic effect). Specifically, Ghosh[55] showed that the changes in M with voltage depended on the Ni content in the $Pd_{1-x}Ni_x$ alloy. M decreased when a negative voltage was applied on $Pd_{74}Ni_{26}$, whereas the opposite behavior was observed on Ni-rich specimens ($Pd_{35}Ni_{65}$). Moreover, the initial value of M in $Pd_{74}Ni_{26}$ could no longer be recovered after cycling for several hours.[55] Non-recovery of the initial mass magnetization, σ_M, was also observed in Pd-Co,[56] where again σ_M did not reach the original value after several cycles. Although the authors pointed to "pure" surface charging as the origin of the observed magnetic changes, some structural changes are likely to occur on the samples as well, particularly after long-term cycling.

The paramagnetic susceptibility of a sintered porous network of interconnected palladium nanocrystallites, electrostatically charged using an electrolyte, was also reported to vary in a reversible manner, due to voltage-induced strain, by Drings *et al.*[57] Subkow and Fähnle[58] provided further theoretical interpretation to the observed effects in nanoporous materials. They demonstrated through *ab initio* simulations that charge accumulation can lead to changes in the surface magnetic anisotropies of the nanoparticles which form the nanoporous network, assuming that only those surfaces that are not at grain boundaries in direct contact with neighboring nanoparticles become charged.

Significantly larger surface charging magnetoelectric effects have been recently observed in Cu-Ni,[18] Co-Pt, and Fe-Pt nanoporous alloys prepared by micelle-assisted electrodeposition, for which the pore wall width could be reduced to 5–7 nm [see Fig. 5(a) for an example of the typical morphology of these films]. The H_C values in these systems could be drastically reduced [by about 25%–32%, as shown in Figs. 5(b) and 5(c)] by properly choosing the sign and strength of the applied voltage (which was generated using an anhydrous propylene carbonate electrolyte containing a low amount of Na^+ and OH^- ions). This reduction in H_C allows for magnetization reversal at significantly lower applied magnetic fields and, therefore, reduces Joule heating effects during writing of the magnetic information. Contrary to the seminal work by Weisheit *et al.*, here the overall thickness of the films could easily exceed 0.5 μm. Similar results were obtained in hierarchically porous Fe-Cu films prepared by electrodeposition on colloidal templated substrates.[19] These results, ascribed to changes in the MAE (as revealed by *ab initio* calculations[18]), are thus very appealing for energy-efficient magnetic actuation. Beyond the unquestionable technological relevance of these results, interesting observations emerge when the behavior of the different investigated nanoporous alloys is compared [Fig. 5(c)]. First, the variations in H_C not always occur for the same voltage polarity. Namely, while H_C in Co-Pt and Fe-Cu decreases for negative applied voltages, H_C in Cu-Ni decreases for positive voltages. On the other hand, only an increase in H_C is observed for Fe-Pt under application of negative voltages. These dissimilar trends for the various investigated alloys might be understood from *ab initio* calculations. For a given crystallographic phase and orientation, the MAE as a function of applied electric field might vary differently with the electric field. Namely, a positive slope in MAE *vs.* electric field was obtained in Co-Pt,[38] whereas a negative slope was found in Cu-Ni.[18] Additionally, the observed effects do not linearly vary with voltage (and in some cases they are only observed for one voltage polarity). This might be due to the dissimilar thicknesses of the ELD which forms when the FM material is negatively or positively polarized as the ion species involved in each case are different. Thus, an asymmetric magnetoelectric effect could actually be anticipated due to the dependence of the EDL structure on the sign of the applied voltage. Further experiments are required to shed light on these issues.

Simultaneously to all these studies on metallic FM alloys, Yamada and coauthors[49] demonstrated for the first time that electric field could be used to manipulate the magnetic properties of a diluted semiconductor whose T_C is above room temperature. The selected material was Co-doped TiO_2, and voltage was applied through the formation of an EDL. The authors demonstrated the same effects using two different electrolytes: the ionic liquid DEME-TFSI and polyethylene oxide with dissolved $CsClO_4$. Through Anomalous Hall Effect (AHE) measurements, they showed that by applying few volts ($V_{applied}$ < 4 V), a clear FM hysteresis loop emerged from the initial paramagnetic signal of the sample. This FM signal, which could not be due to sample FM impurities, scaled with the applied voltage. Moreover, the authors showed a non-monotonic dependence of T_C with the carrier density.

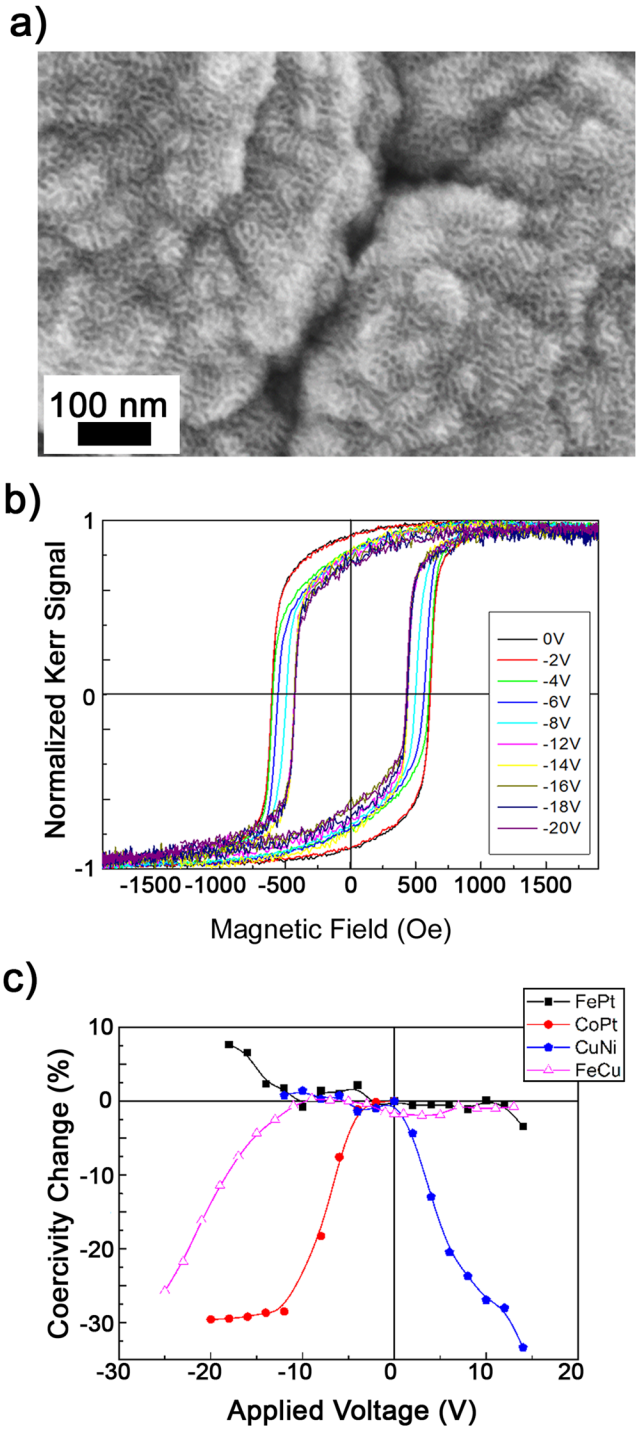

FIG. 5. (a) Typical morphology of a nanoporous Co-Pt film prepared by micelle-assisted electrodeposition, as evidenced by high-resolution scanning electron microscopy (HR-SEM) (on-top view), and (b) hysteresis loops corresponding to nanoporous Co-Pt films, measured under voltage application while the sample remains immersed in propylene carbonate with solvated Na^+ and OH^- ions in solution. (c) Relative changes in coercivity for different nanoporous metallic alloys prepared by electrodeposition, i.e., Fe-Pt, Co-Pt, Cu-Ni,[10] and Fe-Cu.[11] In all cases, the effects are mainly ascribed to surface charge accumulation.

By means of EDL gating using the ionic liquid EMI-TFSI, a drastic tuning of T_C in a cobalt ultra-thin film was demonstrated by Shimamura *et al.*[59] By simply applying ±2 V, the authors demonstrated that T_C could be modified up to 100 K, hence drastically altering the magnetic properties of the film. Not only changes in M, H_C, or T_C have been obtained through electrolyte gating. Herrera and colleagues showed, for example, that the domain wall (DW) dynamics of a FePt thin film can be tailored with an external electric field.[60] Namely, the number of magnetic domains can be increased (and their size decreased) by applying a negative voltage due to a strengthening of the magnetic anisotropy. Conversely, upon positive voltage, a de-pinning of the domain walls was observed due to the reduction in the magnetic anisotropy. In turn, Liu *et al.*[61,62] showed that the DW velocity in CoFeB/MgO/HfO_2 and CoFeB/MgO can be also tailored using an electric field applied through an ionic liquid gate. Specifically, the velocity increases for positive voltages, while negative voltages tend to reduce it. The observed modulation scales by a factor 4.2 using relatively small applied voltages (±0.8 V). A reorientation of the magnetic easy axis with voltage, from perpendicular-to-plane to in-plane with voltage, was also reported by these authors. This is an interesting effect for voltage-driven MRAM applications.

Besides the aforementioned studies dealing with magnetic metallic alloys and semiconductors, there are also a few reports on magnetoelectrically actuated lanthanum strontium manganite ($La_{1-x}Sr_xMnO_3$ or LMSO),[63–65] a ceramic perovskite-type oxide material with a complex phase diagram that exhibits doping-dependent metal-to-insulator and paramagnetic-to-FM transitions (e.g., for certain compositions, these oxides show a high electric conductivity at high temperatures). Voltage-induced carrier doping in LMSO was first reported to modify the $Mn^{4+}/(Mn^{3+} + Mn^{4+})$ ratio, resulting in changes in M close to T_C[63] and the eventual generation of hard magnetic and insulating regions embedded in a soft magnetic matrix (i.e., a phase transition) that could enable four-state memory devices.[64] More recently, Molinari *et al.*[65,66] have shown the possibility to tune the magnetic properties of manganite-based supercapacitors using the ionic liquid DEME-TFSI as an electrolyte. In a film consisting of 3 nm thick $La_{0.74}Sr_{0.26}MnO_3$ with T_C = 246 K, electric charging at T = 235 K induces changes in the manganese oxidation state, altering the spin-spin interactions and leading to a reversible suppression of ferromagnetism.[65] The authors have reported that by tuning the potential window, M can be tuned in-phase and anti-phase, thus opening avenues for this material to be used in transducers. A synergetic effect between electrostatic surface charging (electric-double-layer capacitance) and electrochemical (pseudocapacitance) doping [i.e., arising from chemisorptions of DEME and TFSI ions to the $La_{1-x}Sr_xMnO_3$ (LSMO) surface] has been shown to lead to large changes in M for this system (by 33%), even at room temperature, with relatively small external voltages, of the order of a few V.[66] Remarkably, the properties of LMSO can be also tuned by Li^+ ion intercalation, as it will be discussed in Sec. III C.

Finally, interesting recent studies have explored the possibility of using ionic gels (comprising, e.g., EMIM-TFSI ionic liquid and PVDF dissolved in dimethylformamide and acetone baked at 45 °C) as electrolytes for solid-state systems (i.e., for flexible, wearable electronic devices).[67–69] Zhao *et al.* reported changes in the perpendicular anisotropy of [Pt/Co] multilayers, including a reorientation toward the in-plane direction, with voltage values as low as 4 V.[59] Variations in the RKKY interactions have been also observed in synthetic antiferromagnets using an analogous methodology.[69] In turn, Wang *et al.*[68] demonstrated reversible and non-volatile changes in magnetic anisotropy in Pt/Fe/Pt trilayers directly deposited onto a polyimide flexible substrate after applying 1.8 V.

B. Surface redox reactions using oxidizing electrolytes

Electrochemical reactions have also been proposed as a means for tuning the magnetic properties of materials. The concept relies on exploiting (whenever possible, reversibly) oxidation-reduction reactions of a starting metallic (or metal oxide) material in the presence of an aqueous alkaline electrolyte. A charge-transfer reaction between the electrolyte and the material leads to changes in the oxidation state of the metal (or oxidized metal). As a result, variations in the resulting magnetic properties, typically M, are achieved. Compared to *pure* surface charge accumulation phenomena, wherein only the topmost atomic layers are involved, redox reactions may affect a higher volume of the material. Although oxidation-reduction reactions are set to occur at the surface level, the thickness affected is of the order of several nanometers, and therefore the changes observed tend to be larger.

Concerning the measurement setup, a three-electrode cell filled with an alkaline electrolyte, commonly KOH in a concentration ranging from 0.01M to 1M, is utilized in most of the studies (see Table II). In order to accurately record changes in the magnetic properties of the material while oxidation-reduction reactions take place, the cyclic voltammetry (CV) technique is combined *in situ* with either SQUID magnetometry, AHE, or MOKE. This allows for a direct correlation between redox processes and variations in the magnetic properties of the material under study.

Among the FM metals and alloys subjected to voltage-control of M through electrochemical reactions, iron-based electrodes are the most exploited by far. For example, the electrochemical reduction of magnetite to metallic iron in strong alkaline solutions has been intensively studied by CV[70] because the process of reduction is advantageous for several applications like catalysis, batteries, recycling of metal scraps, and regeneration of corroded steel surfaces. The pathway from iron oxide to metallic iron (and vice versa) and thus the potentials at which the different intermediate species form are relatively well known, and this has encouraged the community working in magnetoelectric phenomena to take Fe-based materials as candidate electrodes for electrochemical-control of their magnetic properties.

Leistner and co-workers studied a 10 nm thick sputtered iron film in KOH at various concentrations (0.001M–6M) by combined CV with AHE measurements.[22] The starting Fe film already contained a thin oxide/hydroxide passivation layer which was reduced by polarization at –1.3 V vs. Standard

calomel electrode (SCE) for 10 min before the experiments were initiated. The authors concluded that 1M KOH was the optimal concentration in order to enable reduction toward metallic Fe upon negative polarization and avoid severe dissolution (and hence, irreversibility) with positive polarization in the potential window between −1.4 V and −0.2 V vs. SCE. A variation of the saturation magnetization (ΔM_S) up to 20% was achieved when the potential was switched from −1.26 V to −0.18 V *vs.* SCE, which was attributed to the re-oxidation of the *ca.* 2 nm thick Fe layer.

Similarly, the occurrence of naturally passivated Fe surfaces was exploited in a following study from Leistner's group.[23,24] Here, the authors studied more sophisticated architectures consisting of [Fe_3O_4/Fe/(001) $L1_0$ FePt] trilayers and FeO_x/Fe nanoislands in 1M KOH, wherein the topmost iron oxide layer was naturally formed on the as-sputtered Fe thin film. The presence of the permanent FePt underlayer, with perpendicular magnetic anisotropy, allowed for changes in the average magnetization orientation and switching from rigid magnet to exchange spring magnet regime (the latter thanks to the Fe/FePt interface). The electroreduction of the Fe_3O_4 layer to metallic Fe caused an increase in the overall thickness of the metallic Fe and its decrease when the polarization was reversed. As a result, M, the remanence-to-saturation magnetization ratio (M_R/M_S), and the perpendicular magnetic anisotropy could be reversibly tuned. An almost ON–OFF voltage-induced magnetic transition was observed in the nanoislands for relatively thin structures[23] (see Fig. 6).

In a different study, Topolovec *et al.*[25] followed the changes in the magnetic moment of γ-Fe_2O_3 (maghemite)

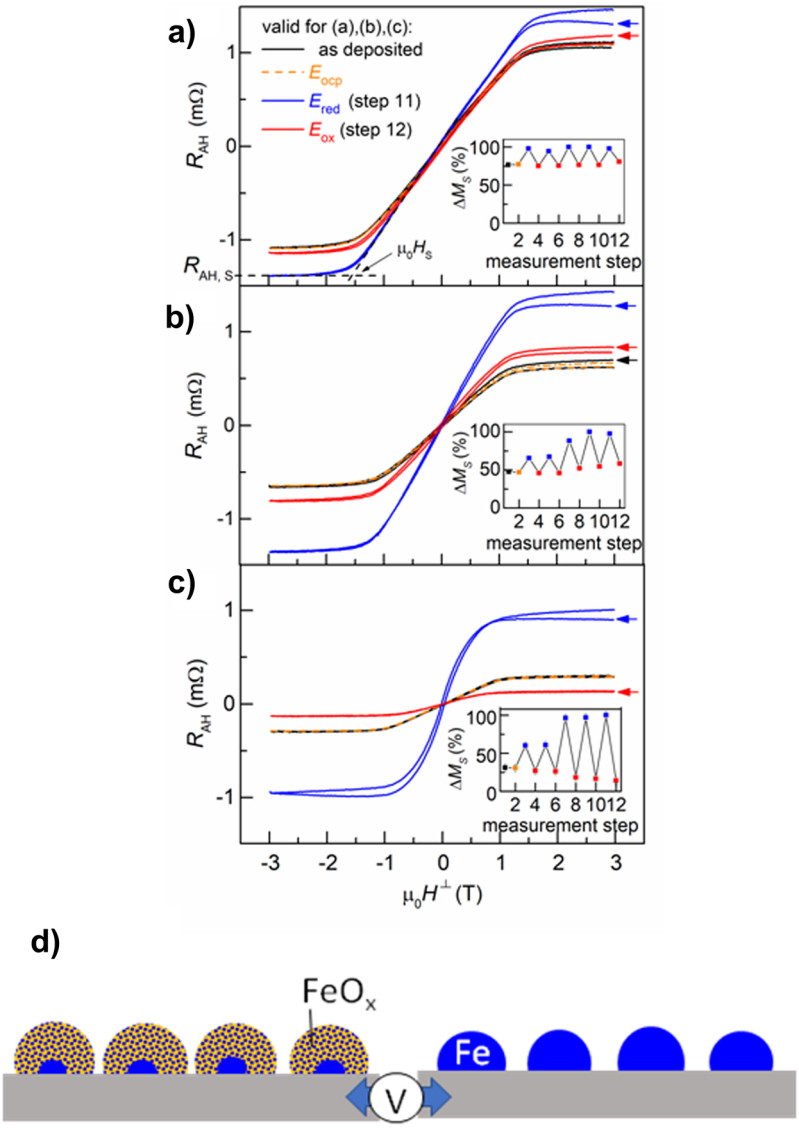

FIG. 6. Magnetization curves as measured by AHE for FeO_x/Fe nanoislands with layer thicknesses of (a) 11 nm, (b) 7 nm, and (c) 4 nm in the as-deposited state and in 1 mol L^{-1} KOH at E_{ocp} (open circuit potential, with no external applied voltage), E_{ox} (oxidizing potential of −0.2 V_{SCE}, potential with respect to a saturated calomel reference electrode), and E_{red} (reduction potential of −1.26 V_{SCE}). The insets depict the relative E-induced changes in M_S. Panel (d) indicates that by applying suitable voltage values to the system, FeO_x can be essentially reduced to Fe, thus resulting in drastic changes in M_S (maximized for the smaller layer thickness, i.e., inset of panel c). Reprinted with permission from Duschek *et al.*, J. Mater. Chem. C **6**, 8411 (2018). Copyright 2018 Royal Society of Chemistry.

nanoparticles (4 nm in size) previously mixed with commercial Pt nanoparticles and pressed into a pellet. A 4% change in the magnetic moment was observed in a 1M KOH medium during combined CV-SQUID magnetometry studies under an applied field of 5 kOe at 300 K. Such a change was not due to any chemical interaction at the γ-Fe_2O_3/Pt interface level but was solely ascribed to the γ-Fe_2O_3 nanoparticles. In particular, the authors observed an increase in M upon negative charging and a decrease in it with positive charging, within the potential window between −650 mV and +300 mV vs. the Au wire quasi-reference electrode. The changes were reversible and ascribed to the formation of Fe_3O_4 upon negative biasing, which would make M to increase. Aside from the chemically induced variation of M, electronic contributions, namely, charging-induced of the magnetic anisotropy and magnetoelastic coupling, could not be ruled out. A further increase in M (up to 10.4%) had been observed in the same material, also by Würschum's team, when bringing the system to the percolation limit,[71] although a detailed correlation between the ongoing electrochemical processes and magnetic behavior is provided in Ref. 25.

Besides Fe-based materials, the influence of electrochemically driven changes in the magnetic response of Co and Pd-Ni alloys has also been investigated. For example, Allongue's team observed a variation of the magnetic anisotropy (K_S) in a Co ultra-thin film produced by electrodeposition on Au (111)/Si(111) substrates. The resulting epitaxial Co(0001)/Au(111) specimens were treated in 0.01M KOH to reversibly oxidize the Co surface, and the changes in K_S were followed by MOKE and further confirmed by density functional theory calculations. An increase in K_S value by 0.36 erg cm^{-2} was attributed to the formation of a Co-OH layer from the initially reduced 3.1 ML Co-H material (i.e., H was proven to be adsorbed onto the Co surface). Electrochemically speaking, this structural change accounted for an electrochemical charge passed through the system of 0.4 mC cm^{-2}.[20]

With the same philosophy, Ghosh[21] ascribed the reversible changes in M for a nanoporous $Pd_{67}Ni_{33}$ alloy to hydrogenation phenomena. In this case, the electrode was fabricated by consolidating $Pd_{67}Ni_{33}$ nanoparticles of ca. 6 nm in diameter into a disk shape and monitorized when immersed in 1M KOH by using a physical property measurement system (PPMS) or VSM magnetometry and CV. Observed changes in the mass magnetization up to 24.6% with negative biasing were attributed to hydrogen absorption (i.e., incorporation of atomic hydrogen in the Pd-Ni lattice). Meanwhile, almost no changes were observed upon positive biasing due to the formation of an antiferromagnetic NiO passivation layer at the surface of the porous $Pd_{67}Ni_{33}$ disk.

Interesting magnetoelectric effects have been reported recently by Quintana *et al.*[72] in single-phase (face-centered cubic) $Cu_{20}Ni_{80}$ (at. %) solid solution alloy films (with sub-10 nm pore size) immersed in a 1M NaOH aqueous solution. Contrary to previous expectations, this system shows an increase (rather than a decrease) in the M_S (up to 33% enhancement with respect to the as-prepared sample) after oxidation (i.e., applying positive voltages). The effect was ascribed to the selectivity of the electrochemical redox processes. Namely, the oxidation of the Cu-Ni film mainly occurred on the Cu counterpart of the solid solution, resulting in a Ni-enriched alloy, thus with a higher M_S. After applying small negative voltages (e.g., −2 V), Cu was reincorporated back into the Cu-Ni solid solution (i.e., not forming any secondary phase), resulting in a reduction in M_S back to its initial value, hence allowing for a full reversibility of the process.

Finally, it is worth mentioning that in some cases, redox reactions also occur even when no aqueous electrolytes are used. For example, Reichel *et al.*[73] reported drastic changes in the magnetic properties of ultra-thin CoPt films when immersed and electrolyte-gated using $LiClO_4$ in dimethyl carbonate-ethylene carbonate.

C. Magneto-ionics and ion intercalation

Magneto-ionics is a very generic term that has been traditionally utilized to describe the propagation of electromagnetic waves by an ionized medium in the presence of an external magnetic field (e.g., the Earth magnetic field).[74] In recent years, this term has been applied to refer to voltage-driven ionic motion (i.e., ion diffusion) in magnetic materials. Most frequently, magneto-ionic effects have been studied in oxide-containing systems. In this case, the material itself includes the source of structural oxygen. Namely, it consists of either an oxide layer or a heterostructure that comprises oxide counterparts which act as donors or acceptors of oxygen. This is different from Sec. III B, where the described redox reactions involved oxygen coming from the surroundings (e.g., oxidative liquid media) and affected mainly the surface of the magnetic material (i.e., oxygen ions did not necessarily diffuse deep toward the interior of the studied system). Furthermore, in addition to oxygen, there are ion migration processes in which other species (e.g., Li^+ ions) are used to tune the magnetic properties. This phenomenon is termed "ion intercalation" in this section.

Bauer *et al.*[28] were the first to use the term "magneto-ionic control" to describe voltage-induced oxygen transport in magnetic films. Namely, they demonstrated that, in Co/GdO_x bilayers, oxygen migration (and, thus, interfacial oxygen chemistry) could be controlled with electric voltage, allowing for a modulation of magnetic properties (in this case, perpendicular magnetic anisotropy) to an extent never achieved before by any other magnetoelectric means.[28] In this case, voltage actuation was carried out in a solid state configuration and GdO_x was the ionic conductor (solid electrolyte) used to provide the oxygen ions. Similarly, Bi *et al.*[27] showed that the easy axis of a thin Co film could be tuned with voltage when Co was grown in contact with GdO_x. These studies stem from previous results from Schellekens *et al.*,[75] Bauer *et al.*,[30,76] Chiba *et al.*,[77] and Bernand-Mantel *et al.*[78] who had demonstrated that domain wall motion in magnetic films and nanowires could be tuned with electric field using AlO_x or GdO_x gating. Magnetic domains could be effectively trapped (pinned) in certain regions of the nanowires taking advantage of this effect.[76] Gilbert *et al.*[29] performed depth-profile structural and magnetic analyses, using polarized neutron reflectometry, to understand how the depth-dependent oxygen diffusion affects the magnetic properties of a relatively thick

(15 nm) Co layer deposited onto AlO_x/GdO_x. In this case, the authors demonstrated that magnetization was tailored along the first 10 nm and that the process was reversible up to a 92%. Zhou *et al.*[32] used HfO_2 with an ionic liquid deposited on top to tune the magnetic properties of a Co/Ni bilayer. Very recently, Tan *et al.*[79] have demonstrated that different ambient conditions (e.g., presence of oxygen or hydrogen in the atmosphere during magneto-ionic experiments in Co/GdO_x bilayers) can lead to very dissimilar magneto-ionic effects, opening the door for H^+ pumping controlled spin orbitronic devices. Voltage-driven oxygen transport across the interface between HfO_2 and Co/Ni resulted in partial oxidation of the metals, leading to the formation of antiferromagnetic oxides (NiO_x and CoO_x) and non-volatile changes in the magnetic properties. An exchange bias effect (loop shift) was observed at low temperatures, which depended on the thickness of the voltage-induced antiferromagnetic oxide layers. Electric-field reversible tuning of T_C and M_S at low temperature (measured by Hall resistance) was also observed by Yan *et al.*[31] in $Co/Ni/HfO_2$ structures with a frozen ionic liquid (which still maintains the electric double layer even while being in the solid state). In this work, variations in the d orbitals of Co, driven by voltage, were also claimed to influence the resulting magnetic properties, besides the ionic migration effects. Control of positive exchange bias using voltage was demonstrated by Gilbert *et al.*[80] in $Gd_xFe_{1-x}/NiCoO$ bilayer films, taking advantage of the strong oxygen affinity of gadolinium. Reversible electric field control of exchange bias is very appealing for energy-efficient spintronic devices. Magneto-ionic control of the coercivity of Co ultra-thin films deposited onto SiO_2 and gated using an inorganic polymer was demonstrated by Tan *et al.*[81] A maximum variation up to 68% was achieved by this means, and the effect was ascribed to oxygen ions' migration from the SiO_2 substrate to the Co films. The utilization of an inorganic polymer (MaN2401) as an insulating layer for electric field control is of particular interest to overcome the formation of pinholes in conventional oxides (which, if grown by atomic layer deposition, require of thermal heating and relatively long deposition times) and also to avoid sophisticated encapsulation techniques that are required if ionic liquids are to be implemented into real spintronic devices.

The antiferromagnetic to FM transition in ultrathin FeRh films deposited on MgO (100) substrates and capped with HfO_2 has also been successfully modified by electrical manipulation using ionic liquid-gating through the reversible transport of oxygen ions, supplied by the HfO_2 layer, across the interface with FeRh.[82] Also interesting is the control of the magnetic properties of LMSO films (40 nm thick), coated with Gd capping layers, through interfacial oxygen migration.[83] Even without applying voltage, oxygen is leached from the film and a Gd_2O_3 layer is formed, leading to changes in M and anisotropy that affect the overall thickness of the film. Similarly, the ionic distributions in $(La,Sr)CoO_3$ films (36 nm thick) could also be controlled in the solid-state by depositing a Gd capping layer and subsequent application of voltage.[84] The observed trends in M and magnetoresistance suggested a significant voltage-driven phase separation, in which metallic FM regions and oxygen-deficient, insulating, non-ferromagnetic regions would co-exist forming percolated networks.

Next we focus on voltage-induced oxygen migration phenomena in magnetic materials which are gated using non-aqueous electrolytes, including ionic liquids (see Table III), without the assistance of GdO_x, HfO_2, or analogous adjacent layers. Similar to the work by Bauer *et al.*,[28] the room temperature perpendicular magnetic anisotropy of SiO_2/Co films could be controllably modified by Zhao *et al.*[85] by means of electric-field-induced O transport, where an initial ultra-thin cobalt oxide layer between Co and the ionic liquid provided the oxygen ions. The superparamagnetic blocking temperature in Cu/Ni ultrathin films (presumably exhibiting Ni/Cu intermixing or containing Ni clusters onto the Cu layer) could be tuned by 28 °C with voltage, using N,N,N-trimethyl-N-propylammonium ($TMPA^+$) and bis(trifluoromethylsulfonyl)imide ($TFSI^-$) as ionic liquid.[86]

Large magneto-ionic effects (leading to changes as high as 20% for M_S and beyond 100% for H_C) were reported in nanoporous Fe-Cu films prepared by sputtering and electrochemical dealloying, when immersed in propylene carbonate (i.e., in an anhydrous electrolyte).[87] In this case, the large observed magnetic changes were caused by controlled and reversible electric-field-driven nanoscale phase transformations between face-centered cubic (*fcc*) and body-centered cubic (*bcc*) structures. These phase transitions were in turn due to selective redox reactions induced by the applied voltage. The oxygen in the sample presumably came in small amounts from the OH^- ions in solution in the propylene carbonate although an oxide passivation layer was probably also formed at the surface of the samples following the synthesis since they were stored in air.

Very recently, Quintana *et al.*[26] reported voltage-driven O and Co redistribution in 100 nm-thick Co_3O_4 films through electrolyte-gating using propylene carbonate, allowing for the controlled generation and suppression of ferromagnetism. A negative voltage reduced Co_3O_4 to Co (ferromagnetism: ON), whereas the process could be reversed by applying a positive bias, aimed at oxidizing Co back to Co_3O_4 (paramagnetism: OFF). These gate-induced O and Co migrations were driven by mixed vacancy clusters as evidenced by positron annihilation spectroscopy. Ionic transport was promoted at grain boundaries and further assisted by the formation of diffusion channels that incorporated large amounts of O. The process was self-sustained in the sense that no external source/sink of oxygen is required (Fig. 7).

Also remarkable are the recent results by Navarro-Senent *et al.*[88] on nanoporous CoPt + CoO_x microdisks, electrolyte-gated using propylene carbonate, in which magnetoelectric effects between the metallic and the oxide counterparts have been found to reduce the H_C by 88% and the Kerr signal amplitude by 60%. This material combined (i) enhanced electrostatic charge accumulation at the surface of the ultra-thin nanopore walls comprised in the micro-disks together and (ii) magneto-ionic phenomena, where voltage-driven O^{2-} migration promoted a partial and controlled reduction from CoO to Co. The effects were found to be reversible but with a relatively slow dynamics.

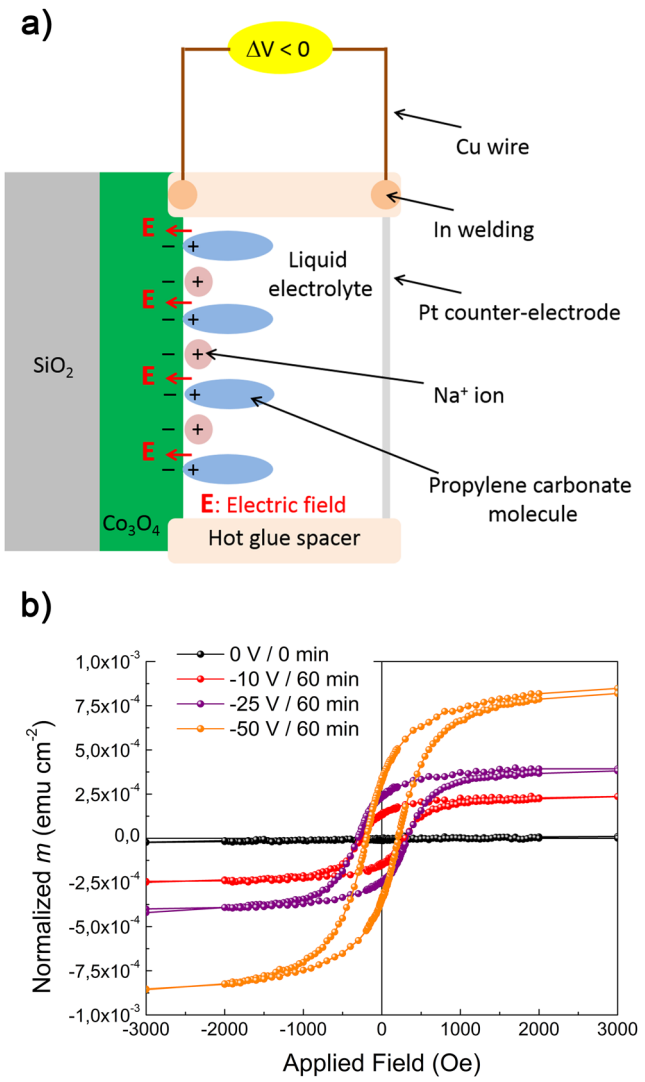

FIG. 7. (a) Schematic illustration of the wire connection to apply voltage on a Co_3O_4 film, grown by atomic layer deposition, in which Cu wires were attached to the sample using indium. The welding was performed at the Co_3O_4 surface. Insulating hot glue spacers were used to avoid short-circuits during VSM measurements.[18] (b) Hysteresis loop recording for this system under application of voltage using a propylene carbonate electrolyte. Although the sample is initially not magnetic [black curve in (b)], a clear ferromagnetic hysteresis loop emerges when the film is subjected to the action of a negative electric field (OFF → ON magnetic transition). Reprinted with permission from Quintana *et al.*, ACS Nano **12**, 10291 (2018). Copyright 2018 American Chemical Society.

In ionically gated $SrRuO_3$ thin films, the onset of ferromagnetism could be reversibly modulated by voltage-induced oxygen migration in $SrRuO_3$ (i.e., by the creation and annihilation of oxygen vacancies in the $SrRuO_3$ lattice). The transition temperature could be decreased up to around 30 K for small positive voltages and, then, recovered when applying the same voltage value but with opposite polarity.[89] Remarkably, in this context of ionic liquid-gating, Lu *et al.* showed that, on top of voltage-driven oxygen migration, hydrogen transport could also be activated by electric fields and in an independent manner from the O diffusion. This dual-ion migration allowed for reversible phase transformations among three different material phases: the perovskite $SrCoO_{3-\delta}$ (FM), the brownmillerite $SrCoO_{2.5}$ (antiferromagnetic), and $HSrCoO_{2.5}$ (weakly FM), hence for an electric-field control of three different magnetic ground states.[90] Interesting results were also reported in electrolyte-gated $SrTiO_3$[91] and $La_{0.5}Sr_{0.5}CoO_{3-\delta}$.[92] In the first case, the authors could discriminate between pure charging, reversible, magnetoelectric effects (for low applied voltage), and persistent electrochemical processes for voltages larger than 3.75 V.[91] Walter *et al.*[92] showed that mixed electrostatic and redox mechanisms occur in $La_{0.5}Sr_{0.5}CoO_{3-\delta}$ depending on the voltage polarity. Magnetoelectric effects were also reported in cobaltite/manganite ($SrCoO_{3-x}/La_{0.45}Sr_{0.55}MnO_{3-y}$) heterostructures, where a reversible manipulation of oxygen vacancies using DEME-TFSI ionic liquid was shown to result in magnetic phase transitions and drastic changes in H_C, exchange bias field, and T_C.[93] Walter *et al.*[94] also showed that ionic gels can be effectively used to tailor the magnetic properties of $La_{0.5}Sr_{0.5}CoO_{3-\delta}$ using voltage values of the order of a few V, which are sufficient to induce changes in the oxygen vacancy density, as evidenced using synchrotron hard x-ray diffraction and polarized neutron reflectometry. Dhoot *et al.*[95] reported a transition from a ferromagnetic metal to an insulating ground state with positive voltage in $La_{0.8}Ca_{0.2}MnO_3$ films gated using EMIM:TFSI. This resulted in changes in the colossal magnetoresistance values, which were found to be reversible upon changing the polarity of the applied voltage. Similar to all the aforementioned examples, a pronounced electric-field effect was demonstrated in phase-separated $Pr_{0.65}(Ca_{0.75}Sr_{0.25})_{0.35}MnO_3$ thin films, particularly at low temperatures, using DEME-TFSI as electrolyte (electric double layer transistor). The effect of the electric field in this material couples with that of the applied magnetic field, leading to pronounced changes in electroresistance and magnetoresistance at around 80 K. The effects were ascribed to an increase in the ferromagnetic fraction in this oxide manganite film.[96] Analogously, changes in the magnetic properties of $Pr_{1-x}(Ca_{1-y}Sr_y)_xMnO_3$ were also reported by Hatano *et al.*, again using the electric double layer transistor with an ionic liquid. The electric field was found to drastically change the temperature-dependence of the electric resistivity and, concomitantly, had an effect on the metal (FM)-to-insulator transition.[97]

Based on previous knowledge from Li-ion batteries and supercapacitors, non-oxidative lithium based electrolytes have also been employed for magnetoelectric purposes. For instance, Leistner *et al.*[98] used a non-aqueous $LiPF_6$-based electrolyte and observed that the magnetic moment of FePt films could be tuned by reversible O ion transport coming from the native iron oxide surface layer. Based on this work, Leistner *et al.*[99] further investigated voltage-driven O transport in electrolyte-gated FePt/iron oxide composites where a reversible change in M_S and magnetic anisotropy was

achieved. In these studies, though, Li^+ ions were not intercalated in the structure of the investigated materials.

Ions other than oxygen can also be controllably inserted or extracted by means of electric fields to tailor magnetic properties of materials. In fact, increasing the number of transferrable ion species is of great benefit to enrich material functionalities. Due to its crucial role in batteries, Li has been commonly chosen as the mobile specie to migrate in some magnetoelectric studies. Typically, the mobile Li^+ ions are provided by non-aqueous organic liquids containing $LiPF_6$. For example, Dasgupta *et al.*[100] showed that the magnetic properties of maghemite (γ-Fe_2O_3) can be controllably tuned in a reversible manner by voltage-induced Li insertion or extraction. More recently, Zhang *et al.*[34] demonstrated electric-field-driven lithiation (magnetic moment enhancement)/delithiation (magnetic moment suppression) of nanoscale α-Fe_2O_3-based batteries, enabling strong ferromagnetism as an extra degree of freedom in the field of energy storage. Similarly, voltage-driven Li^+ ion intercalation has been recently shown to be effective to tune the M values of nanoporous $Co_{0.5}Ni_{0.5}Fe_2O_4$ and $CoFe_2O_4$ by roughly 5% and 2.5%, respectively, in a rather reversible manner, using 20 wt. % LiTFSI dissolved in EMIM-TFSI as an electrolyte in a potential window 1.5–3.3 V.[101] The authors obtained larger variations in M by extending the potential window to 1.1–3.4 V, but then the effects were highly irreversible.

Besides the aforementioned oxides, Li^+ intercalation was also studied in α-$LiFe_5O_8$ mesoporous thin films using LiTFSI in EMIM-TFSI as electrolyte. This spinel ferrite could reversibly store Li^+ in a potential ranging from 3.2 to 1.4 V. The electrochemical reactions proceeded in a topotactic way, which allowed control and tuning of M at room temperature (up to 4%) in a reversible manner.[102] Finally, oxygen deficient $LiFe_5O_{8-x}$ was used as a target ferrimagnetic material in which magnetic properties were tailored by voltage, in the solid state, at the nanoscale, taking advantage of the relatively low activation energy of this oxide for Li^+ ion migration.[103] Li^+ de-intercalation/intercalation resulted in changes in the resistive switching properties of this oxide, as well as in the magnetic domain pattern (imaged by magnetic force microscopy) and M.

D. Electrolyte-gated ferroelectric/ferromagnetic heterostructures

This section is devoted to electrolyte-gated heterostructured multiferroic materials, which mainly refer to FE/FM bilayers actuated using liquid electrolytes (e.g., ionic liquids). Conventionally, most of the investigated multiferroic heterostructures used for electric-field control of magnetism, in fact, do not incorporate electrolytes on their systems. For this reason, electrolyte-assisted control of magnetism in multiferroic structures is still considered to be rather underexplored.

In general terms (not necessarily actuated using electrolytes), the most widely studied FE/FM systems encompass $La_{1-x}Sr_xMnO_3$ (LSMO) or $La_{1-x}Ca_xMn_{O3}$ (LCMO) combined with FE $BaTiO_3$ (BTO) or $Pb(Zr_{0.2}Ti_{0.8})O_3$ (PZT), commonly known as FM-FE perovskite oxide heterostructures.[40,104] The underlying magnetoelectric mechanisms in these multiferroic heterostructures comprise variations of the charge accumulation (and, in turn, the FE polarization) that lead to changes in strain or chemical bonding at the FE/FM interface. An effective way to polarize FE polymer films is to use electrolytes (including aqueous ones) since the formation of the EDL aids to polarize the FE counterpart in a controlled manner.[105]

Herklotz and co-workers demonstrated the reversible control of interfacial magnetism in a LSMO and PZT multiferroic heterostructure through ionic-liquid assisted FE switching.[106] They pointed out that the use of ionic-liquid for switching the FE polarization provides several advantages, which include (i) its feasibility to thinner FE films since the leakage currents are smaller through the ionic liquid and (ii) the ionic liquid allows a reversible *in situ* switching of the FE polarization in large areas of the FE while avoiding the risk of pinholes compared to the common metallic top electrodes. The authors concluded that the origin of the enhancement/reduction in the interfacial magnetization in this system relied on the hole accumulation/depletion produced by the FE polarization.

Similarly, Nishino *et al.*[107] reported the use of an ionic liquid for the switching of the PZT polarization aiming at a FE control of the transport properties in $SrRuO_3$ and Nb-doped $SrRuO_3$. The ionic liquid was used in order to promote the formation of an EDL at the interface between the FE (PZT) and the ionic liquid, which was very effective for inducing polarization reversal in the FE. Interestingly, although the study was focused on the modulation of the carrier density in $SrRuO_3$, a change in T_C was observed, from 115 K to 90 K.

As mentioned in the introduction, in multiferroic materials, the ME effect can be induced in both directions (i.e., either voltage can tune the magnetic properties of the FM or a change in the electrical response of the FE can be induced by means of a magnetic field applied to the FM). Based on the latter idea, Chau *et al.*[108] studied the magnetoelectric effect (changes in charge density induced by applied magnetic fields) in Terfenol-D (FM)/PZT (FE)/electrolyte-polymer matrix composite materials. They demonstrated that the presence of the electrolytic-polymer matrix increases the magnetoelectric coefficient compared to heterostructures with conventional insulating matrices. Even though the aim of the work was not the control of magnetism, the results suggest that such a system could be a potential candidate for electrolyte-gated magnetoelectric actuation.

IV. APPLICATIONS, CHALLENGES, AND FUTURE PROSPECTS

In recent years, exciting new results in the field of electrolyte-gated magnetoelectric actuation have been obtained in metallic, semiconducting, and dielectric oxide thin films and nanoporous structures. At present, there is a huge potential to use these materials in a variety of innovative applications, such as energy-efficient spintronic devices (e.g., tunnel junctions in voltage-driven MRAMs) or multistate magnetic memories.[40] These applications go beyond the conventional utilization of magnetoelectricity[109] in magnetic

actuators, transducers, or, more recently, energy harvesters.[110] Furthermore, new avenues have been opened recently on the utilization of magnetoelectric heterostructures in biomedicine, for example for wireless electric stimulation of cells (e.g., osteoblasts or neurons)[111–113] or to enhance the effectiveness of drug delivery.[114,115] In these latter cases, magnetoelectric actuation is performed in liquid media although in most applications (*e.g.*, physical ones), all-solid configurations are preferred. Nonetheless, the use of liquid electrolytes offers important advantages: (i) an enhanced ion mobility (compared to solid electrolytes), which allows for ion intercalation (penetration of ions from the electrolyte toward the material of interest), (ii) generation of ultra-high electric fields (due to the very narrow thickness of the EDL) at the surface of the magnetic material, and (iii) possibility to easily penetrate inside 3D nanoporous magnetic alloys and oxides, hence allowing for a more effective electric surface charging and eventual redox or magneto-ionics effects.

There are some challenges that need to be overcome in order to fully exploit the technological applications of state-of-the-art magnetoelectric materials. First, it is important to induce all these effects at room temperature. Therefore, further magnetoelectric studies on new types of diluted magnetic semiconductors with T_C above room temperature need to be performed in order to take advantage of this class of materials. Also important is to be able to induce magneto-ionic effects in solid-state devices without thermally assisted ionic diffusion. That is, ion migration should occur at room temperature, without heating.

There is also a need to decrease the required voltage values to a level below the breakdown threshold of the dielectric layer. The insulating oxide layers are typically made relatively thick and defect-free to avoid leakage currents. However, the increase in the barrier thickness causes a reduction in the effective electric field. To overcome this problem, electrolyte-gating using ionic liquids turns out to be a very promising strategy to achieve very large electric fields for relatively low applied voltages (due to the ultra-narrow thickness of the EDL). The role of structural defects at the interface with the electrolyte needs to be further assessed in order to optimize magnetoelectric actuation. Also important is to minimize mechanical fatigue effects under repetitive electric cycling, which can be substantial in FM/FE bilayers or voltage-actuated nanoporous oxides immersed in liquid electrolytes (i.e., electrostriction).

Depending on the end application, the type of magnetoelectric actuation and materials need to be chosen adequately. For instance, surface charging is, in principle, instantaneous and might be very appropriate for spintronics. But, at the same time, the induced effects are volatile, unless they are mediated by a FE layer (with a remanent electric polarization). Magneto-ionics typically results in permanent magnetoelectric effects (*i.e.*, that remain upon removal of the applied voltage). So, this phenomenon could be used in magnetic memories. However, since magneto-ionics relies on ionic migration, this effect is still exceedingly slow for practical applications. Further progress in this particular topic could be achieved with a better control of the microstructure of the layers or by purposely introducing structural defects (*i.e.*, ion irradiation).

In general, the mechanisms responsible for magnetoelectric actuation are still rather poorly understood and are often more complex than as initially anticipated. This hinders deeper control of the voltage-driven changes in the magnetic properties. As an example, "pure" surface charging effects turn out to not to be always instantaneous and, what is even worse, they are not always fully reversible and reproducible after long-term cycling (see Table I), hence suggesting structural changes at the surface of the magnetic materials of interest. Further in-depth structural investigations, preferably using *in situ* surface characterization techniques, are, therefore, urgently needed.

Progress beyond the state-of-the-art in the use of magnetoelectric materials for spintronics and magnetic memory devices would certainly benefit from the implementation of all-solid configurations, either by using solid ionic conductors as dielectrics (such as Gd_2O_3 or HfO_2) or organic ferroelectrics (*e.g.*, PVDF). In the case of nanoporous magnetic alloys, the latter might be more convenient since polymer precursors might penetrate more easily inside the small pores when compared to oxide dielectrics although recent progress has been also made on coating the inner surfaces of nanoporous magnetic alloys with dielectric oxides using atomic layer deposition.[116]

ACKNOWLEDGMENTS

This work was funded by the European Research Council under the SPIN-PORICS 2014-Consolidator Grant (Agreement No. 648454), the Generalitat de Catalunya (2017-SGR-292 project), the Spanish Government (No. MAT2017-86357-C3-1-R and associated FEDER project), and the European Union's Horizon 2020 research and innovation programme under the Marie Skłodowska-Curie Grant Agreement No. 665919. E.P. acknowledges the Ramon y Cajal (No. RYC-2012-10839) fellowship from MINECO.

REFERENCES

[1] D. Giles, *Introduction to Magnetism and Magnetic Materials* (CRC Press, Taylor & Francis Group, Boca Raton, Florida, USA, 2016).
[2] B. Dieny, R. C. Sousa, J. Hérault, C. Papusoi, G. Prenat, U. Ebels, D. Houssameddine, B. Rodmacq, S. Auffret, and L. D. Buda-Prejbeanu, Int. J. Nanotechnol. **7**, 591 (2010).
[3] P. Curie, J. Phys. Theor. Appl. **3**, 393 (1894).
[4] D. N. Astrov, J. Exp. Theor. Phys. **38**, 708 (1960).
[5] Y. Wang, J. Hu, Y. Lin, and C.-W. Nan, NPG Asia Mater. **2**, 61 (2010).
[6] N. Lei, T. Devolder, G. Agnus, P. Aubert, L. Daniel, J.-V. Kim, W. Zhao, T. Trypiniotis, R. P. Cowburn, C. Chappert, D. Ravelosona, and P. Lecoeur, Nat. Commun. **4**, 1378 (2013).
[7] P. M. Shepley, A. W. Rushforth, M. Wang, G. Burnell, and T. A. Moore, Sci. Rep. **5**, 7921 (2015).
[8] Z. Huang, I. Stolichnov, A. Bernand-Mantel, J. Borrel, S. Auffret, G. Gaudin, O. Boulle, S. Pizzini, L. Ranno, L. Herrera Diez, and N. Setter, Appl. Phys. Lett. **103**, 222902 (2013).
[9] T. H. E. Lahtinen, K. J. A. Franke, and S. van Dijken, Sci. Rep. **2**, 258 (2012).
[10] W. Eerenstein, N. D. Mathur, and J. F. Scott, Nature **442**, 759 (2006).

[11]J. A. Mundy, C. M. Brooks, M. E. Holtz, J. A. Moyer, H. Das, A. F. Rébola, J. T. Heron, J. D. Clarkson, S. M. Disseler, Z. Liu, A. Farhan, R. Held, R. Hovden, E. Padgett, Q. Mao, H. Paik, R. Misra, L. F. Kourkoutis, E. Arenholz, A. Scholl, J. A. Borchers, W. D. Ratcliff, R. Ramesh, C. J. Fennie, P. Schiffer, D. A. Muller, and D. G. Schlom, Nature **537**, 523 (2016).
[12]H. Ohno, D. Chiba, F. Matsukura, T. Omiya, E. Abe, T. Dietl, Y. Ohno, and K. Ohtani, Nature **408**, 944 (2000).
[13]D. Chiba, M. Yamanouchi, F. Matsukura, and H. Ohno, Science **301**, 943 (2003).
[14]M. Weisheit, S. Fähler, A. Marty, Y. Souche, C. Poinsignon, and D. Givord, Science **315**, 349 (2007).
[15]T. Maruyama, Y. Shiota, T. Nozaki, K. Ohta, N. Toda, M. Mizuguchi, A. A. Tulapurkar, T. Shinjo, M. Shiraishi, S. Mizukami, Y. Ando, and Y. Suzuki, Nat. Nanotechnol. **4**, 158 (2009).
[16]D. Chiba, S. Fukami, K. Shimamura, N. Ishiwata, K. Kobayashi, and T. Ono, Nat. Mater. **10**, 853 (2011).
[17]C. Black and J. Welser, IEEE Trans. Electron Devices **46**, 776 (1999).
[18]A. Quintana, J. Zhang, E. Isaraín-Chávez, E. Menéndez, R. Cuadrado, R. Robles, M. D. Baró, M. Guerrero, S. Pané, B. J. Nelson, C. M. Müller, P. Ordejón, J. Nogués, E. Pellicer, and J. Sort, Adv. Funct. Mater. **27**, 1701904 (2017).
[19]E. Dislaki, S. Robbennolt, M. Campoy-Quiles, J. Nogués, E. Pellicer, and J. Sort, Adv. Sci. **5**, 1800499 (2018).
[20]N. Di, J. Kubal, Z. Zeng, J. Greeley, F. Maroun, and P. Allongue, Appl. Phys. Lett. **106**, 122405 (2015).
[21]S. Ghosh, J. Mater. Res. **28**, 3010 (2013).
[22]K. Duschek, M. Uhlemann, H. Schlörb, K. Nielsch, and K. Leistner, Electrochem. Commun. **72**, 153 (2016).
[23]K. Duschek, A. Petr, J. Zehner, K. Nielschn, and K. Leistner, J. Mater. Chem. C **6**, 8411 (2018).
[24]K. Duschek, D. Pohl, S. Fähler, K. Nielsch, and K. Leistner, APL Mater. **4**, 032301 (2016).
[25]S. Topolovec, P. Jerabek, D. V. Szabó, H. Krenn, and R. Würschum, J. Magn. Magn. Mater. **329**, 43 (2013).
[26]A. Quintana, E. Menéndez, M. O. Liedke, M. Butterling, A. Wagner, V. Sireus, P. Torruella, S. Estradé, F. Peiró, J. Dendooven, C. Detavernier, P. D. Murray, D. A. Gilbert, K. Liu, E. Pellicer, J. Nogues, and J. Sort, ACS Nano **12**, 10291 (2018).
[27]C. Bi, Y. Liu, T. Newhouse-Illige, M. Xu, M. Rosales, J. W. Freeland, O. Mryasov, S. Zhang, S. G. E. te Velthuis, and W. G. Wang, Phys. Rev. Lett. **113**, 267202 (2014).
[28]U. Bauer, L. Yao, A. J. Tan, P. Agrawal, S. Emori, H. L. Tuller, S. van Dijken, and G. S. D. Beach, Nat. Mater. **14**, 174 (2015).
[29]D. A. Gilbert, A. J. Grutter, E. Arenholz, K. Liu, B. J. Kirby, J. A. Borchers, and B. B. Maranville, Nat. Commun. **7**, 12264 (2016).
[30]U. Bauer, S. Emori, and G. S. D. Beach, Appl. Phys. Lett. **100**, 192408 (2012).
[31]Y. N. Yan, X. J. Zhou, F. Li, B. Cui, Y. Y. Wang, G. Y. Wang, F. Pan, and C. Song, Appl. Phys. Lett. **107**, 122407 (2015).
[32]X. Zhou, Y. Yan, M. Jiang, B. Cui, F. Pan, and C. Song, J. Phys. Chem. C **120**, 1633 (2016).
[33]X. Chen, X. Zhu, W. Xiao, G. Liu, Y. P. Feng, J. Ding, and R.-W. Li, ACS Nano **9**, 4210 (2015).
[34]Q. Zhang, X. Luo, L. Wang, L. Zhang, B. Khalid, J. Gong, and H. Wu, Nano Lett. **16**, 583 (2016).
[35]S. Dasgupta, B. Das, Q. Li, D. Wang, T. T. Baby, S. Indris, M. Knapp, H. Ehrenberg, K. Fink, R. Kruk, and H. Hahn, Adv. Funct. Mater. **26**, 7507 (2016).
[36]G. Wei, G. L. Wei, D. Wang, Y. Chen, Y. Tian, S. Yan, L. Mei, and J. Jiao, Sci. Rep. **7**, 12554 (2017).
[37]G. Wei, L. Wei, D. Wang, Y. Chen, Y. Tian, S. Yan, L. Mei, and J. Jiao, Appl. Phys. Lett. **110**, 062404 (2017).
[38]O. O. Brovko, P. Ruiz-Díaz, T. R. Dasa, and V. S. Stepanyuk, J. Phys.: Condens. Matter **26**, 093001 (2014).
[39]C. Song, B. Cui, F. Li, X. Zhou, and F. Pan, Prog. Mater. Sci. **87**, 33 (2017).
[40]S. Fusil, V. Garcia, A. Barthélémy, and M. Bibes, Annu. Rev. Mater. Res. **44**, 91 (2014).
[41]I. Stolichnov, S. W. E. Riester, H. J. Trodahl, N. Setter, A. W. Rushforth, K. W. Edmonds, R. P. Campion, C. T. Foxon, B. L. Gallagher, and T. Jungwirth, Nat. Mater. **7**, 464 (2008).
[42]A. Mardana, S. Ducharme, and S. Adenwalla, Nano Lett. **11**, 3862 (2011).
[43]H. Zhan , J. Cervenka, S. Prawer, and D. J. Garrett, J. Phys. Chem. C **121**, 4760 (2017).
[44]H.-J. Butt, K. Graf, and M. Kappl, *Physics and Chemistry of Interfaces* (Wiley-VCH Verlag GmbH & Co. KGaA, 2003), pp. 42–56.
[45]K. Bohinc, V. Kralj-Iglic, and A. Iglic, Electrochim. Acta **46**, 3033 (2001).
[46]S. Grimnes and Ø. Martinsen, *Bioimpedance and Bioelectricity Basics*, 3rd ed. (Elsevier, 2015), e-book.
[47]R. J. Hunter, *Foundations of Colloid Science* (Oxford University Press, Oxford; New York, 2001).
[48]E. M. Ney, C.-H. Hou, and P. Taboada-Serrano, J. Chem. Eng. Data, **63**, 2557 (2018).
[49]Y. Yamada, K. Ueno, T. Fukumura, H. T. Yuan, H. Shimotani, Y. Iwasa, L. Gu, S. Tsukimoto, Y. Ikuhara, and M. Kawasaki, Science **332**, 1065 (2011).
[50]M. Zhernenkov, M. R. Fitzsimmons, J. Chlistunoff, J. Majewski, I. Tusoda, and E. E. Fullerton, Phys. Rev. B **82**, 024420 (2010).
[51]A. Obinata, Y. Hibino, D. Hayakawa, T. Koyama, K. Miwa, S. Ono, and D. Chiba, Sci. Rep. **5**, 14303 (2015).
[52]Q. Yang, L. Wang, Z. Zhou, L. Wang, Y. Zhang, S. Zhao, G. Dong, Y. Cheng, T. Min, Z. Hu, W. Chen, K. Xia, and M. Liu, Nat. Commun. **9**, 991 (2018).
[53]A. K. Mishra, C. Bansal, M. Ghafari, R. Kruk, and H. Hahn, Phys. Rev. B **81**, 155452 (2010).
[54]J. Weissmüller, R. N. Viswanath, D. Kramer, P. Zimmer, R. Würschum, and H. Gleiter, Science **300**, 312 (2003).
[55]S. Ghosh, J. Magn. Magn. Mater. **323**, 552 (2011).
[56]S. Ghosh, C. Lemier, and J. Weissmüller, IEEE Trans. Magn. **42**, 3617 (2006).
[57]H. Drings, R. N. Viswanath, D. Kramer, C. Lemier, J. Weissmüller, and R. Würschum, Appl. Phys. Lett. **88**, 253103 (2006).
[58]S. Subkow and M. Fähnle, Phys. Rev. B **84**, 220409(R) (2011).
[59]K. Shimamura, D. Chiba, S. Ono, S. Fukami, N. Ishiwata, M. Kawaguchi, K. Kobayashi, and T. Ono, Appl. Phys. Lett. **100**, 122402 (2012).
[60]L. Herrera Diez, A. Bernand-Mantel, L. Vila, P. Warin, A. Marty, S. Ono, D. Givord, and L. Ranno, Appl. Phys. Lett. **104**, 082413 (2014).
[61]Y. T. Liu, S. Ono, G. Agnus, J.-P. Adam, S. Jaiswal, J. Langer, B. Ocker, D. Ravelosona, and L. Herrera Diez, J. Appl. Phys. **122**, 133907 (2017).
[62]Y. T. Liu, G. Agnus, S. Ono, L. Ranno, A. Bernand-Mantel, R. Soucaille, J.-P. Adam, J. Langer, B. Ocker, D. Ravelosona, and L. Herrera Diez, J. Appl. Phys. **120**, 023901 (2016).
[63]A. K. Mishra, A. J. Darbandi, P. M. Leufke, R. Kruk, and H. Hahn, J. Appl. Phys. **113**, 033913 (2013).
[64]B. Cui, C. Song, G. Wang, Y. Yan, J. Peng, J. Miao, H. Mao, F. Li, C. Chen, F. Zeng, and F. Pan, Adv. Funct. Mater. **24**, 7233 (2014).
[65]A. Molinari, H. Hahn, and R. Kruk, Adv. Mater. **30**, 1703908 (2018).
[66]A. Molinari, P. M. Leufke, C. Reitz, S. Dasgupta, R. Witte, R. Kruk, and H. Hahn, Nat. Commun. **8**, 15339 (2017).
[67]S. Zhao, Z. Zhou, C. Li, B. Peng, Z. Hu, and M. Liu, ACS Nano **12**, 7167 (2018).
[68]C. Wang, H. Zhang, C. Li, Y. He, L. Zhang, X. Zhao, Q. Yang, D. Xian, Q. Mao, B. Peng, Z. Zhou, W. Cui, and Z. Hu, ACS Appl. Mater. Interfaces **10**, 29750 (2018).
[69]Q. Yang, Z. Zhou, L. Wang, H. Zhang, Y. Cheng, Z. Hu, B. Peng, and M. Liu, Adv. Mater. **30**, 1800449 (2018).
[70]J. F. Monteiro, Y. A. Ivanova, A. V. Kovalevsky, D. K. Ivanou, and J. R. Frade, Eletrochim. Acta **193**, 284 (2016).
[71]T. Traubnig, S. Topolovec, K. Nadeem, D. V. Szabó, H. Krenn, and R. Würschum, Phys. Status Solidi RRL **5**, 150 (2011).

[72]A. Quintana, E. Menéndez, E. Isaraín-Chavez, J. Fornell, P. Solsona, F. Fauth, M. D. Baró, J. Nogués, E. Pellicer, and J. Sort, Small **14**, 1704396 (2018).
[73]L. Reichel, S. Oswald, S. Fähler, L. Schultz, and K. Leistner, J. Appl. Phys. **113**, 143904 (2013).
[74]H. G. Booker, Proc. R. Soc. London, Ser. A **150**, 267 (1935).
[75]A. Schellekens, A. van den Brink, J. Franken, H. Swagten, and B. Koopmans, Nat. Commun. **3**, 847 (2012).
[76]U. Bauer, S. Emori, and G. S. D. Beach, Nat. Nanotechnol. **8**, 411 (2013).
[77]D. Chiba, M. Kawaguchi, S. Fukami, N. Ishiwata, K. Shimamura, K. Kobayashi, and T. Ono, Nat. Commun. **3**, 888 (2012).
[78]A. Bernand-Mantel, L. Herrera-Diez, L. Ranno, S. Pizzini, J. Vogel, D. Givord, S. Auffret, O. Boulle, I. M. Miron, and G. Gaudin, Appl. Phys. Lett. **102**, 122406 (2013).
[79]A. J. Tan, M. Huang, C. O. Avci, F. Büttner, M. Mann, W. Hu, C. Mazzoli, S. Wilkins, H. L. Tuller, and G. S. D. Beach, Nat. Mater. **18**, 35 (2019).
[80]D. A. Gilbert, J. Olamit, R. K. Dumas, B. J. Kirby, A. J. Grutter, B. B. Maranville, E. Arenholz, J. A. Borchers, and K. Liu, Nat. Commun. **7**, 11050 (2016).
[81]F. N. Tan, G. J. Lim, W. C. Law, F. L. Luo, H. X. Liu, F. Poh, D. Shum, and W. S. Lew, J. Phys. D: Appl. Phys. **51**, 365001 (2018).
[82]M. Jiang, X. Z. Chen, X. J. Zhou, B. Cui, Y. N. Yan, H. Q. Wu, F. Pan, and C. Song, Appl. Phys. Lett. **108**, 202404 (2016).
[83]A. J. Grutter, D. A. Gilbert, U. S. Alaan, E. Arenholz, B. B. Maranville, J. A. Borchers, Y. Suzuki, K. Liu, and B. J. Kirby, Appl. Phys. Lett. **108**, 082405 (2016).
[84]D. A. Gilbert, A. J. Grutter, P. D. Murray, R. V. Chopdekar, A. M. Kane, A. L. Ionin, M. S. Lee, S. R. Spurgeon, B. J. Kirby, B. B. Maranville, A. T. N'Diaye, A. Mehta, E. Arenholz, K. Liu, Y. Takamura, and J. A. Borchers, Phys. Rev. Mater. **2**, 104402 (2018).
[85]S. Zhao, Z. Zhou, B. Peng, M. Zhu, M. Feng, Q. Yang, Y. Yan, W. Ren, Z.-G. Ye, Y. Liu, and M. Liu, Adv. Mater. **29**, 1606478 (2017).
[86]K. T. Yamada, T. Koyama, H. Kakizakai, K. Miwa, F. Ando, M. Ishibashi, K.-J. Kim, T. Moriyama, S. Ono, D. Chiba, and T. Ono, Appl. Phys. Express **10**, 013004 (2017).
[87]S. Robbennolt, A. Quintana, E. Pellicer, and J. Sort, Nanoscale **10**, 14570 (2018).
[88]C. Navarro-Senent, J. Fornell, E. Isarain-Chávez, A. Quintana, E. Menén-dez, M. Foerster, L. Aballe, E. Weschke, J. Nogues, E. Pellicer, and J. Sort, ACS Appl. Mater. Interfaces **10**, 44897 (2018).
[89]H. T. Yi, B. Gao, W. Xie, S.-W. Cheong, and V. Podzorov, Sci. Rep. **4**, 6604 (2014).
[90]N. Lu, P. Zhang, Q. Zhang, R. Qiao, Q. He, H.-B. Li, Y. Wang, J. Guo, D. Zhang, Z. Duan, Z. Li, M. Wang, S. Yang, M. Yan, E. Arenholz, S. Zhou, W. Yang, L. Gu, C.-W. Nan, J. Wu, Y. Tokura, and P. Yu, Nature **546**, 124 (2017).
[91]K. Ueno, H. Shimotani, Y. Iwasa, and M. Kawasaki, Appl. Phys. Lett. **96**, 252107 (2010).
[92]J. Walter, H. Wang, B. Luo, C. D. Frisbie, and C. Leighton, ACS Nano **10**, 7799 (2016).
[93]B. Cui, C. Song, F. Li, X. Y. Zhong, Z. C. Wang, P. Werner, Y. D. Gu, H. Q. Wu, M. S. Saleem, S. S. P. Parkin, and F. Pan, Phys. Rev. Appl. **8**, 044007 (2017).
[94]J. Walter, G. Yu, B. Yu, A. Grutter, B. Kirby, J. Borchers, Z. Zhang, H. Zhou, T. Birol, M. Greven, and C. Leighton, Phys. Rev. Mater. **1**, 071403(R) (2017).
[95]A. S. Dhoot, C. Israel, X. Moya, N. D. Mathur, and R. H. Friend, Phys. Rev. Lett. **102**, 136402 (2009).
[96]J. Lourembam, J. Wu, J. Ding, W. Lin, and T. Wu, Phys. Rev. B **89**, 014425 (2014).
[97]T. Hatano, Z. Sheng, M. Nakamura, M. Nakano, M. Kawasaki, Y. Iwasa, and Y. Tokura, Adv. Mater. **26**, 2874 (2014).
[98]K. Leistner, N. Lange, J. Hänisch, S. Oswald, F. Scheiba, S. Fähler, H. Schlörb, and L. Schultz, Electrochim. Acta **81**, 330 (2012).
[99]K. Leistner, J. Wunderwald, N. Lange, S. Oswald, M. Richter, H. Zhang, L. Schultz, and S. Fähler, Phys. Rev. B **87**, 224411 (2013).
[100]S. Dasgupta, B. Das, M. Knapp, R. A. Brand, H. Ehrenberg, R. Kruk, and H. Hahn, Adv. Mater. **26**, 4639 (2014).
[101]L. A. Dubraja, C. Reitz, L. Velasco, R. Witte, R. Kruk, H. Hahn, and T. Brezesinski, ACS Appl. Nano Mater. **1**, 65 (2018).
[102]C. Reitz, C. Suchomski, D. Wang, H. Hahnad, and T. Brezesinski, J. Mater. Chem. C **4**, 8889 (2016).
[103]X. Zhu, J. Zhou, L. Chen, S. Guo, G. Liu, R.-W. Li, and W. D. Lu, Adv. Mater. **28**, 7658 (2016).
[104]F. Matsukura, Y. Tokura, and H. Ohno, Nat. Nanotechnol. **10**, 209 (2015).
[105]H. Toss, N. Sani, S. Fabiano, D. T. Simon, R. Forchheimer, and M. Berggren, J. Phys.: Condens. Matter **28**, 105901 (2016).
[106]A. Herklotz, E.-J. Guo, A. T. Wong, T. L. Meyer, S. Dai, T. Z. Ward, H. N. Lee, and M. R. Fitzsimmons, Nano Lett. **17**, 1665 (2017).
[107]R. Nishino, Y. Kozuka, F. Kagawa, M. Uchida, and M. Kawasaki, Appl. Phys. Lett. **113**, 143501 (2018).
[108]K. H. Chau, Y. W. Wonga, and F. G. Shin, Appl. Phys. Lett. **94**, 202902 (2009).
[109]L. E. Fuentes-Cobas, J. A. Matutes-Aquino, M. E. Botello-Zubiate, A. González-Vázquez, M. E. Fuentes-Moreno, and D. Chateigner, in *Advances in Magnetoelectric Materials and their Application*, Handbook of Magnetic Materials, edited by K. H. J. Buschow (Elsevier, 2015), Vol. 24, Chap. 3, p. 237.
[110]A. Lasheras, J. Gutiérrez, S. Reis, D. Sousa, M. Silva, P. Martins, S. Lanceros-Mendez, J. M. Barandiarán, D. A. Shishkin, and A. P. Potapov, Smart Mater. Struct. **24**, 065024 (2015).
[111]C. Ribeiro, V. Correia, P. Martins, F. M. Gama, and S. Lanceros-Mendez, Colloids Surf., B **140**, 430 (2016).
[112]X.-Z. Chen, N. Shamsudhin, M. Hoop, R. Pieters, E. Siringil, M. S. Sakar, B. J. Nelson, and S. Pané, Mater. Horiz. **3**, 113 (2016).
[113]X.-Z. Chen, M. Hoop, N. Shamsudhin, T. Huang, B. Özkale, Q. Li, E. Siringil, F. Mushtaq, L. D. Tizio, B. J. Nelson, and S. Pané, Adv. Mater. **29**, 1605458 (2017).
[114]M. Nair, R. Guduru, P. Liang, J. Hong, V. Sagar, and S. Khizroev, Nat. Commun. **4**, 1707 (2013).
[115]A. Rodzinski, R. Guduru, P. Liang, A. Hadjikhani, T. Stewart, E. Stimphil, C. Runowicz, R. Cote, N. Altman, R. Datar, and S. Khizroev, Sci. Rep. **6**, 20867 (2016).
[116]J. Zhang, A. Quintana, E. Menéndez, M. Coll, E. Pellicer, and J. Sort, ACS Appl. Mater. Interfaces **10**, 14877 (2018).